3 July 2019

Dear Dr. Romano,

We thank you and the reviewers for your comments, and we are pleased to submit a revised version of "**Global sinusoidal seasonality in precipitation isotopes**" for consideration at HESS. We found the reviewers' comments to be helpful in making adjustments to better communicate our science. We remain confident that the data product we develop here is in high demand by the hydrology community (and broader communities), as many have been inquiring about the availability of this presented work.

We have now uploaded the precipitation isotope maps to a Zenodo repository (meeting FAIR standards). We have opted to take this approach, rather than uploading the grids as supplemental data (as we previously proposed) because this is more adaptable and allows for larger files. We will lift the restrictions once the paper is accepted so that the data products are fully available.

Please see the attached responses to reviewers, descriptions of revisions, and tracked changes.

Sincerely, on behalf of coauthors,

Scott T. Allen
Postdoctoral Research Associate
University of Utah
Spatiotemporal Isotope Analytics Lab (SPATIAL)

Our responses below are in black, Time's New Roman and referee's comments are in blue, Calibri font.

Response to Referee #1

General comments: This manuscript describes a method to determine sine curve fits to the seasonal cycle of precipitation isotopes from stations around the globe. Interpolated maps of seasonality and a database of sine curve parameters were produced (not available for review). Overall the paper is well written, but ambitious in scope. The paper lacks an adequate explanation of how this work advances upon previous work, and needs more attention to sources of uncertainty in the analysis. With these improvements, the results presented here should be a solid contribution to the field of isotope hydrology.

Thank you for your feedback. We will now better explain the differences between our research and others' related research. To clarify, our paper allows readers to immediately understand the location and strength of seasonal cycles in precipitation isotopes. Perhaps most importantly, our method provides information (i.e. sine curve parameters) that is not directly available from isomap.org or the online isotopes in precipitation calculator (OIPC), but is increasingly used in isotope hydrology (e.g., young water fraction calculations).

In the revised draft, we better explain what this data product offers and what limitations it has (see comments below as well as responses to reviewer 2). Indeed sine curves do not perfectly represent precipitation isotope variability; they are, however, a useful metric to visualize and describe presence, strength, and timing of seasonality. Understanding where these patterns occur aids in guiding future studies' analytical approaches. We have also added an additional uncertainty analysis (see comments below).

Specific comments:

Abstract: this is somewhat disorganized, and would be improved by aiming toward a straightforward description of the problem or question addressed, the analyses done, and the significance of the result.

In rereading our abstract, we realize that some confusion could arise because it is hard to discern between results and methods (because the paper does focus on methodology). We believe that this is warranted because we are producing a data product, and thus the results often justify subsequent methodological steps. Nonetheless, we have revised the manuscript to make it adhere to a more typical structure.

P 2 L 4-10: Authors note that interpretive studies may ignore either the spatial or temporal aspect of the isotopic signal. Please explain further how the current approach improves on the interpolated seasonal data that are already available, where mean monthly isotope values can be downloaded from an online calculator for a set of spatial coordinates (isoscapes.org). The advancement represented by the approach in the current manuscript needs to be clearly described.

In our method, we first capture the seasonal cycle, and then interpolate. We now specify that difference and its importance as an advance on current methods. Secondly, our analysis is a next-level data product, mostly intended for specific hydrology applications (although others are discussed later). One can quickly look up how amplitudes vary using our study, which would require many steps

using isomap.org data. Since publishing Allen et al 2018, many people have asked for the product that we are here providing because completing these sine fits can be tricky (e.g., with respect to constraining phase values, consistent amplitude definitions, and quantifying errors). We provide these geospatial data with the hope and expectation that other researchers can complete their own studies more efficiently. We have better clarified our specific objectives in the abstract, introduction, and conclusions.

P 4 L 13-15; P10 L 13-14: Amount weighting is important for hydrological interpretations; please discuss whether amount is best included within the sine fitting procedure for an area, or whether amount should be included at the level of a regional or local study, where it would be used to weight the robust-fit seasonal values?

The amount weighting can be important, but we prefer not to say which approach is "best" because the two support different applications. One scenario where amount-weighting is important in the fitting is if there was an anomalously dry month (e.g., 1 small precipitation event), where the storm had atypically high δ18O values, or the sample was exposed to evaporation in the collector. In this scenario, the amplitude would be exaggerated in a non-weighted sine fit. If these values were later weighted a typical amount, it could result in a misrepresentation of the precipitation inputs. In an alternative hypothetical scenario, using weighted fits in a Mediterranean region (with dry summers) might under-represent the true seasonal amplitude. Both metrics are valuable, and we will now further discuss their respective limitations in the methods section (2.2).

P 4 L 20: mean annual precipitation amount globally seems to have low predictive value for isotopic composition (table 2), does this parameter combine rainfall with snow water equivalent (SWE) measurements, and are those accurate enough to make this a useful parameter for station characterization?

Precipitation amount varies by orders of magnitude across the globe; we are only using 1st-order linear regressions, so it is not overly surprising that it does not explain much (and is thereby mostly excluded from the regression equations). As discussed in response to reviewer 2, there is indeed some collinearity among these predictor variables.

While quantifying snowfall inputs can be challenging, it is unlikely to cause errors that are large compared to the range of variation in precipitation amounts across sites. We now specified that SWEs are accounted for.

P 5 L 1-2: are the areas and stations where there is no sinusoidal seasonal cycle clearly denoted in the database?

No they were not, but they will now be made identifiable because the phase term will be replaced with "NA"; the amplitudes and offsets are still useful (as will be described in the manuscript).

Section 2.3: Maps of predicted global precipitation isotope seasonality (sine curve parameters) and precipitation amount were generated with an interpolation scheme. Was any model validation performed by holding back a portion of station data and analyzing differences between measured and predicted isotopic value? This type of assessment should be done for the precipitation isotope seasonality and rainfall amount values.

We remind the reviewer that we are presenting this as a method for predicting seasonal cycles, not for predicting individual monthly values (unlike the sinusoidal model used in Allen et al 2018, which was tested using individual months). We now validate the model's prediction of sine parameters. Individual month values are highly erratic and can deviate substantially from the sine curves (as we show in what is now Figure 2, and formerly S1); there is a whole paragraph dedicated to discussing this point. We have now re-run the model iteratively, holding back subsets of the sites to be used

solely in validation and not in calibration. We will report those values as prediction errors of amplitude, phase, and offset.

P 6 L 15, L26-31, P7 L 1-5: It is not so surprising that tropical locations have seasonal cycles if one considers that land surface temperatures are not the primary control. Feng, X. et al., 2009, JGR, doi:10.1029/2008JD011279 (already cited); Scholl, M. et al., 2009, WRR, doi:10.1029/2008WR007515; Bailey, A. et al., 2017, JGR,doi:10.1002/2016JD026222 may provide a broader understanding of seasonal isotope patterns in the tropics. Condensation/equilibration temperatures can be very low and vapor sources isotopically depleted in tropical regions, where convective precipitation systems (esp. in the ITCZ) reach well above the freezing layer. The position of Hadley cell boundaries seems somewhat overemphasized here; atmospheric circulation factors that control isotope patterns (prevailing winds, atmospheric structure, dominant seasonal weather patterns) - have been identified in isotope-enabled GCM studies for tropical and temperate latitudes.

Thank you for directing us to these papers, which will now be cited in our study. We will expand our discussion of previously described tropical isotope cycles and the role circulation patterns in driving those cycles.

P7L4: Precipitation d-excess globally exhibits a seasonal cycle, please see Pfahl and Sodemann, 2014, doi:10.5194/cp-10-771-2014. We would expect similar behavior for lc-excess, but with a less-distinct amplitude.

Yes, it is well described that seasonal d-excess cycles exist (and we will now cite this reference). However, while d-excess variations can result from variations along a LMWL of slope < 8, LC-excess variations result from systematic seasonal deviations from LMWLs. Thus, we are describing patterns that differ from what is described previously in Pfahl and Sodemann. We will now expand on this difference to clarify.

P 8 L 26-28: "grid-cell means are not always representative of individual station locations, as demonstrated by the mismatch between the elevations of monitoring stations and the mean elevations of the pixels they occupy (Figure S5)". Given that elevation is a major factor in isotopic composition of precipitation, how does this reflect on the interpolation and smoothing used to produce the maps? Should the map result be presented at the global scale, given that authors (appropriately) aim to "produce global maps and data that support stable isotope applications," and "predict individual-month values from a sine curve (P 9 L 6)"? Regional maps, where topography is presumably better represented, would seem to be a better approach and I encourage revision of this paper to include those maps and data sets, or at least a thorough explanation of the process of creating and calibrating regional maps.

The answer to this question obviously depends on application. We shared these same concerns, which is exactly why we pursued this project as we did: a) using a high resolution DEM to conduct the initial interpolation, b) producing the global map, but also carefully showing where it fails to capture individual points, c) processing and sharing the data such that it can be immediately incorporated into regional regression models and d) showing where regional models perform best (Figure 6). Of course, we cannot produce every regional map because we cannot anticipate every future 'region' for which a map might be needed.

Regarding the point-to-cell mismatch, this problem is true of most exercises in which data collected at one scale are interpreted as representative of a larger scale. By conducting the new error analysis described above, we quantify the magnitude of error which is partially due to the problem described here.

We also further emphasize to readers that the ability to "predict individual-month values" from sine curves requires that the R^2 values are high, and not just that there is a seasonal cycle.

P 10 L 5-7: Please identify "regions where "seasonal precipitation isotope dynamics are well described by sine curves," and where they are not, in a table or specific map. This would make the material much more informative to users of the data and prevent improper use of interpolated values. It is important to identify places where sinusoidal cycles cannot be used, especially given the discussion on p. 10 where authors suggest numerous applications for the data.

Previously, information showing how well sine curves capture the monthly variations is in Figure S1. We now move Figure S1 into the main text so that nobody misses this information (Now Figure 2). We now also further describe the limitations and their consequences on Page 10.

P 10 L 26: there are other references for this concept, please improve this section by including citations specific to the biological and geological processes that are noted; to improve the paper organization, consider moving material from lines 5-35 to the introduction, then briefly revisiting here.

We do not agree that it is helpful to lengthen the introduction to then just revisit those points later, as this information is not critical for understanding the basis of the study. Nonetheless, we have improved on this by including relevant citations in the discussion.

P 11: "The *majority* of stable isotope time series measured at 653 precipitation isotope monitoring stations show significant sinusoidal seasonal cycles in precipitation isotopes" and "In Supporting Information 2, we provide fitted sine curves and site metadata for *all* 653 precipitation monitoring stations" ... Given that some of the stations patterns do not have a sinusoidal cycle, why are sine curves being provided for stations where they are not applicable?

This is an excellent point and we will now comment on this in the second-to-last paragraph in the discussion section. Even where there is not a sinusoidal cycle, the sine curve provides a measure of central tendency, which is of value. Also, by providing the sine-fit and parameters, we can show why the curve fit is not 'significant': e.g., short time series, small amplitude, erratic month-to-month values (i.e., leading to a large RMSE). Furthermore, including near-zero amplitudes can be important for fitting regional regression models. The phase term is the only one of the three parameters that is meaningless when the sine curve is not significant. We remove the phase values of non-significant sine curves from the data tables because we cannot think of any application for which those would be useful.

P 11 L 15-20: Supporting information 2 and 3 were not available for peer review and have not been evaluated. In this section, please provide details about the sources of raw data from "publicly available datasets" that were used in this work, with citations, attribution or links, to aid further research by others.

We will provide references in Supporting Information 2. Both files will be made available upon acceptance.

Figure S3 – this is not very informative at the coarse scale shown here - the reasons underlying phase shifts between temperature and isotopes (seasonality) globally are fairly well understood and should be addressed separately for different climate zones, if included at all. Figure 3b provides much the same information.

This is in the supplemental because we also believe that it is not crucial, but potentially helpful or interesting to someone. Thus, we prefer to keep it, but we can enhance it by breaking out below and above 30 degrees latitude sites.

Response to Referee #2

General comments: This paper makes an important contribution to the scientific literature by providing estimates of coefficients of sinusoidal cycles in precipitation isotopic composition at global scale. These estimates are useful for analyses of water transit time and water source attribution in hydrological, biological, and geological studies. Regression models are presented that will allow users characterize precipitation isotope cycles at points or as raster grids.

Specific comments:

P 2: additional information on previous geostatistical analyses (Bowen et al. 2014) and products, such as IsoMAP (http://isomap.org), should be included in the Introduction. Please explain how this study improves on previous work (eg., IsoMAP).

We now further discuss other isotope data products. It is important to note that our analysis yields a very different product: maps that show seasonal cycles, rather than predictions of isotope values in specific months or years (e.g., products from Bowen et al.). Statistically, our approach first extracts the seasonal signal from the data, and then interpolates those signals. As such, the values used in the interpolations are a product of an entire time series, not just single points.

Our paper allows readers to immediately understand the location and strength of seasonal cycles in precipitation isotopes. Perhaps most importantly, our method provides information (i.e. sine curve parameters) that is not directly available from isomap.org or the online isotopes in precipitation calculator (OIPC), but is increasingly used in isotope hydrology (e.g., young water fraction calculations). While products from Bowen et al. could be used for alternative calculations of isotope seasonality, that product is not currently available. We are not critiquing Bowen et al.'s method, we are simply offering a different product for use in hydrological analyses and expect that the product will find uses beyond its obvious intended applications.

We now make these points in the introduction.

P 3 L 3-7: The data set used to develop the regressions is large and potentially veryuseful to other users; however, a link to the data is not readily apparent. The authors indicate there is a compiled data set; however, I was unable to identify a link in the cited reference (Jasechko et al. 2016)(the Methods section of that paper indicates they compiled approximately 63K data points). Readers will not be able to reproduce the analysis in this paper without access to the precipitation isotope sample data. It is essential to provide a clear link to the raw data set (with appropriate citations for data sources).

We now cite the data sources in the data table and update the data availability statement so that it specifies how all of the data can be accessed. It is true that these precipitation data were previously analyzed by Jasechko et al. and were obtained via direct download from the IAEA's database (ref. 34 in Jasechko et al. 2016 and http://www-naweb.iaea.org/napc/ih/IHS_resources_isohis.html) and via personal communication with leaders of two national precipitation isotope networks: S. J. Birks (e.g. see ref. 37 in Jasechko et al. 2016) and J. M. Welker (e.g. see ref. 36 in Jasechko et al. 2016). By providing the fitted sinusoid statistics, this paper marks a step forward because it does provide a single compiled dataset of metrics describing precipitation isotope data.

P 4 L 19: the list of potential explanatory variables is reasonable; however, distance to nearest ocean ignores the influence of prevailing wind direction. While perhaps beyond the scope of this paper, it might be possible to include in future analyses. In the meantime, this source of error could be discussed in the Discussion section.

We now expand our discussion of how circulation patterns and storm trajectories relate to isotope patterns.

P 4 L 24-25: Model parameterization does not appear to follow accepted statistical best practices. In stepwise multiple regression, selection of model parameters usually is based on minimizing the Akaike information criterion (AIC) (Akaike 1981) or Bayesian information criterion (BIC), rather than maximizing R2, which could lead to model overparameterization. Colinearity does not appear to have been considered quantitatively, but should be; it often is tested using the variance inflation factor (VIF) (Hair et al. 2005).

We understand that AIC is commonly used, but in our case, we found that minimizing the AIC led to the selection process retaining more terms than were retained by our method; we now mention this in the manuscript. Note that our method was not solely to maximize R^2 values, because we also excluded all coefficient p-values that were not statistically significant ($p < 0.05$). We now report the VIFs. Even if we hypothetically used all of the potential predictor values (which was never the case), all of VIFs are less than 10 (i.e., a commonly used cutoff value).

P 7 L 4: define LC-excess.

LC-excess is now defined (and Landwehr and Coplen 2006 is cited).

P 8 L 10-15: One of the main contributions of this paper is the presentation of models for amplitude, phase, and offset. This allows readers to estimate these cycle characteristics at other sites and/or create raster grids (as the authors have done). This is worth mentioning explicitly in the Discussion.

We now more clearly emphasize this point.

P 9 L 3-4: cannot locate Supporting Information 2.

We opted to not release our data product until it is clear that it is finalized and the manuscript will be accepted.

Table 1: consider including p-values.

Given the size of the dataset, we prefer to not include p values because they are all extremely small ($p=10^{-6}$ for the weakest of these regression).

References:
Akaike, Hirotugu. 1981. "Likelihood of a model and information criteria."
Journal of Econometrics 16 (1):3-14. doi: 10.1016/0304-4076(81)90071-3.

Bowen, Gabriel J, Zhongfang Liu, Hannah B Vander Zanden, Lan Zhao, and George Takahashi. 2014. "Geographic assignment with stable isotopes in IsoMAP." Methods in Ecology and Evolution 5 (3):201-206.

Hair, J.F., W.C. Black, B. Babin, R. Anderson, and R.L. Tatham. 2005. Multivariate data

analysis. 6th ed. Upper Saddle River, New Jersey: Prentice Hall.

Jasechko, Scott, James W. Kirchner, Jeffrey M. Welker, and Jeffrey J. McDonnell. 2016. "Substantial proportion of global streamflow less than three months old." Nature Geosci 9:126-129. doi: 10.1038/ngeo2636.

Interactive comment on Hydrol. Earth Syst. Sci. Discuss., https://doi.org/10.5194/hess-2019-61, 2019.

Response to Referee #3

The authors present an incredibly useful predictive statistical model of the global patterns of d18O and d2H in precipitation. The methods are adequate and sound and the results are clearly described and presented in tables and figures. In my opinion, the manuscript can be accepted in its present form. I leave the following three comments only to encourage the authors to expand the discussion if they agree it would improve the paper.

The authors' objective to produce the predictive model was clearly motivated by a need in the hydrological community for isotopic input data to calculate young water fractions and unravel storage selection behavior of watersheds using stable isotope data. The observed patterns in explanatory variables are only lightly discussed in terms of atmospheric circulation patterns or origins of atmospheric water vapor.

There are a number of studies that have used atmospheric air mass trajectory analyses to study the variability of isotopes in precipitation. I understand this is well outside the scope of this manuscript - and possibly out of reach computationally. It might be worth mentioning air mass trajectory analysis as a possible path for improving the predictions of stable isotopes in precipitation.

The reviewer is correct that our primary objective is motivated by needs of the hydrologic community. The reviewer is also correct that air-mass trajectory effects could result in some of the scatter in the initial regression models. We now add further discussion on air-mass trajectory effects.

On page 4, the authors describe the decision to use the "robust-fitted" seasonal parameters (as opposed to the "amount-weighted" parameters) for further analysis because they capture the variations during drier seasons better. I wonder if the "amountweighted" offset would provide a better estimate which is less biased by light (summer) precipitation events and if there is a significant difference between the two estimates.

Although we do focus on the robust fitted data in the manuscript, we also provide values for the amount-weighted fits as part of the data products provided. They can be directly compared using the supplemental data that we will now provide. We also have extended the methods section, where we describe the two fitting approaches, to emphasize that these two metrics have different limitations.

Global sinusoidal seasonality in precipitation isotopes

Scott T. Allen[1], Scott Jasechko[2], Wouter R. Berghuijs[1], Jeffrey M. Welker[3,4], Gregory R. Goldsmith[5], James W. Kirchner[1,6,7]

[1]Department of Environmental Systems Science, ETH Zurich, Zurich, 8092, Switzerland.
[2]Bren School of Environmental Science and Management, University of California at Santa Barbara, Santa Barbara, CA, 93117, USA
[3]Ecology and Genetics Research Unit, University of Oulu, Finland and UArctic
[4]Biological Sciences Department, University of Alaska, Anchorage
[5]Schmid College of Science and Technology, Chapman University, Orange CA, 92866, USA
[6]Swiss Federal Research Institute WSL, Birmensdorf, 8903, Switzerland
[7]Department of Earth and Planetary Science, University of California, Berkeley, California, 94709, USA

Correspondence to: Scott T. Allen (scott.t.allen@utah.edu)

Abstract: Quantifying seasonal variations in precipitation δ^2H and δ^{18}O is important for many stable isotope applications, including inferring plant water sources and streamflow ages. Our objective is to develop a data product that ~~Here we present global maps that~~ concisely quantif~~ies~~ies the seasonality of stable isotope ratios in precipitation. We fit sine curves defined by amplitude, phase and offset parameters to quantify annual precipitation isotope cycles at 653 meteorological stations on all seven continents. At most of these stations, including in tropical and subtropical regions, sine curves can represent the seasonal cycles in precipitation isotopes. Additionally, the amplitude, phase, and offset parameters of these sine curves correlate with site climatic and geographic characteristics. Multiple linear regression models based on these site characteristics capture most of the global variation in ~~can map global~~ precipitation isotope amplitudes, ~~phases,~~ and offsets; while phase values were not well predicted by regression models globally, they were captured by zonal (0°-30° and 30°-90°) regressions, which were then used to ~~assemble~~produce global maps. ~~. To produce~~These global maps of sinusoidal seasonality in precipitation isotopes based on regression models were ~~, W~~we then adjusted ~~the~~ for the ~~regression based maps models for~~ residual spatial variations that were not captured by the regression models. The resulting mean ~~Median~~ prediction errors were ~~for amplitude and offset averaged~~0.49 ‰ for δ^{18}O amplitude, 0.73 ‰ ~~δ^{18}O~~for ~~for δ^{18}O amplitude~~ δ^{18}O ~~and~~ offset (and 4.0 ‰ and 7.4 ‰ for δ^2H amplitude and offset), ~~median phase errors were~~8 days for phase values in latitudes outside of 30°, and ~~errors~~20 days for phase values in latitudes inside of 30°. We make the~~se~~ gridded global maps of precipitation δ^2H and δ^{18}O ~~cycles~~seasonality publicly available. We also make tabulated site data and fitted sine curve parameters available to support the development of regionally calibrated models, which ~~will were~~will often be~~generally be~~ more accurate than our global model for regionally specific studies.

1

1 Introduction

Characterizing the stable oxygen ($^{18}O/^{16}O$) and hydrogen ($^{2}H/^{1}H$) isotope compositions of precipitation can provide insights into the temporal and spatial origins of water, and of geological and biological materials that incorporate O and H from water. However, the isotopic composition of precipitation is difficult and costly to measure across large spatial scales or at high temporal frequencies, and thus precipitation isotope measurements are often unavailable for the times and locations at which they are needed. Consequently, compiled precipitation isotope data (e.g., Global Network for Isotopes in Precipitation; International Atomic Energy Agency) and interpolations of mean and monthly precipitation isotope data (e.g., Bowen et al., 2005; Bowen & Wilkinson, 2002) are used across many fields of science (West et al., 2010).

Although these network datasets and interpolated maps contain spatial and temporal information, it is often convenient to simplify and average across one of those dimensions. When identifying the spatial origin of water in a sample, investigators may use spatial patterns in mean isotope ratios (despite those patterns varying temporally and those samples not integrating water signatures throughout years). Additionally, when identifying the temporal origin of water in a sample, investigators often use time-series of isotope data from the nearest measurement location (and thus do not account for spatial differences). Alternatively, concise representations of large-scale spatiotemporal precipitation isotope patterns could be widely useful and mitigate the need to average precipitation isotope data across space or time. Various tools and interpolation schemes exist for predicting precipitation isotope ratios at a ~~place~~given location~~, such as the~~ (e.g., Online Isotopes in Precipitation Calculator (following ~~based on~~ Bowen and Revenaugh, 2003), or for mapping spatial patterns in mean or monthly values over specified intervals (e.g.,~~, such as~~ Isomap.org following (Bowen et al., 2014)~~, .; h~~However, previous methods have not explicitly supported predictions of seasonal isotope cycles by first using metrics that capture isotopic temporal dynamics and then interpolated those metrics.

Isotope ratios in precipitation often follow distinct seasonal cycles that can be approximated by sine curves (Bowen, 2008; Dutton et al., 2005; Feng et al., 2009; Halder et al., 2015; Vachon et al., 2007; Wilkinson and Ivany, 2002)~~(Dutton et al., 2005; Feng et al., 2009; Halder et al., 2015; Vachon et al., 2007; Wilkinson and Ivany, 2002)~~, and the parameters describing those sine curves are often predictable in space (Allen et al., 2018; Jasechko et al., 2016). Sine curves concisely represent temporal dynamics because they express continuous, cyclic time series as functions of only three parameters (*amplitude*, *phase*, and *offset*). To predict isotope seasonality across the globe, values of these three sine parameters, fitted to monthly precipitation isotope data at monitoring stations, can be described as functions of station climate and geography. Such mapped sinusoidal cycles were shown to be effective in predicting monthly precipitation isotope values across Switzerland (Allen et al., 2018). Beyond being useful for predicting isotope values ~~at~~ in specific ~~times~~seasons, sine curves generally aid in characterizing the propagation of cyclic signals. For example, as precipitation travels through hillslopes and into streams, seasonal isotope amplitudes are dampened, reflecting transport processes that can be quantified as a stream-precipitation amplitude ratio

2

(Kirchner, 2016a, 2016b); this *young water fraction*, which requires sine curve fitting of precipitation isotopes, has been used in many recent studies (Clow et al., 2018; von Freyberg et al., 2018; Jacobs et al., 2018; Jasechko et al., 2016, 2017; Lutz et al., 2018; Song et al., 2017). Thus, there are immediate ~~and obvious~~ applications ~~that could use~~for ~~quantified and mappde~~mapped ~~sinusoids~~sine curves that ~~capture~~characterize ~~–~~precipitation isotope cycles across the globe. ~~Thus~~More

5   generally, spatial data describing how precipitation isotope compositions vary seasonally could facilitate interpretations of environmental $^{18}O/^{16}O$ and $^{2}H/^{1}H$ data and support predictions of precipitation isotope compositions in time and space.

Here we present global maps of precipitation isotope cycles that capture patterns in precipitation isotope seasonality. We first describe the strength of seasonal isotope cycles, and quantify how well sine curves explain monthly precipitation measurements

10   at each of 653 precipitation isotope monitoring stations. We then explore how well the parameters describing those sine curves can be predicted across the globe, as a function of site characteristics. Lastly, we produce global maps and data that support stable isotope applications, and make these maps and data publicly available. We conduct these analyses to support a growing need for quantifications of seasonal cycles in precipitation isotopes, not to challenge the methods previously used in other precipitation isotope models.

15   **2. Methods**

2.1. Data

We used a global dataset of monthly precipitation oxygen and hydrogen isotope measurements from 650 and 610 precipitation monitoring stations, respectively. These previously compiled (Jasechko et al., 2016) data were collected from the Canadian Network for Isotopes in Precipitation (Birks and Edwards, 2009; Birks and Gibson, 2013), the US Network for Isotopes in

20   Precipitation (Delavau et al., 2015; Welker, 2000, 2012), and the Global Network for Isotopes in Precipitation (Aggarwal et al., 2011; Halder et al., 2015). ~~Some stations have datasets that are as long as 57 years, although shorter durations are more common (Figure S1a).~~ Following Jasechko et al. (2016), we characterize seasonal cycles only at monitoring stations that report precipitation isotope compositions for at least eight unique months. Monthly precipitation amounts (or snow-water equivalencies) are also available from 623 of the 650 stations that measured oxygen isotope ratios, and from 603 of the 610

25   stations that measured hydrogen isotope ratios. All hydrogen and oxygen isotope ratios of precipitation are denoted as $\delta^{2}H$ and $\delta^{18}O$, defined by

$$\delta^2 H = \frac{(^2H/^1H)_{sample} - (^2H/^1H)_{V-SMOW}}{(^2H/^1H)_{V-SMOW}} \times 1000\ ‰\ ,\quad (1)$$

and

$$\delta^{18} O = \frac{(^{18}O/^{16}O)_{sample} - (^{18}O/^{16}O)_{V-SMOW}}{(^{18}O/^{16}O)_{V-SMOW}} \times 1000\ ‰\ ,\qquad (2)$$

30   where *V-SMOW* refers to the Vienna Standard Mean Ocean Water standard.

3

We compiled gridded climatological and geographical data for global modelling and for inferring site characteristics of the precipitation monitoring stations (Figure 1). We downloaded climate maps of monthly precipitation sums and monthly means of daily low, high, and mean temperature, all at 5-arc-minute (i.e., 0.083°) resolution (WorldClim; Fick & Hijmans, 2017). Station climate data were inferred from these gridded products for all but three stations that were on small islands or stationary weather vessels, for which local meteorological data were acquired. The range of mean monthly temperatures was computed at each pixel (and each monitoring station) as the difference between the highest and lowest monthly mean values, using the WorldClim data. Annual mean daily temperature range was calculated as the mean differences between daily minimum and maximum temperatures. The WorldClim data were also used to calculate time of peak precipitation and temperature, and seasonal amplitude of precipitation and temperature, metrics which can together capture global patterns in hydroclimate (Berghuijs and Woods, 2016). We also used a 30-second gridded elevation map (GTOPO30; US Geological Survey, 1996) that was aggregated to 5-minutes for consistency with the other grids. Monitoring station elevation data were not inferred from the grids, but instead downloaded directly from the isotope network databases. Distance from oceans and seas was calculated in ArcGIS 10.4.1 (ESRI, Redlands, USA) using published coastline data (Wessel and Smith, 1996) for the centre of each 5-minute pixel and for each monitoring station.

2.2. Sine-fitting methods

We fitted sine curves (described by the parameters *amplitude*, *phase*, and *offset*) to each monitoring station's monthly measured δ^{18}O and δ^2H time series using a nonlinear fitting routine ("fitnlm" in MATLAB R2016B, Mathworks, Natick, Massachusetts, USA). The sine curve is defined with a fixed period of one year,

$$\text{Precipitation } \delta^{18}\text{O or } \delta^2\text{H } (t) = amplitude \times \sin(2\pi t - phase) + offset \ , \quad (3)$$

where t is the fractional year. All fitted amplitudes and phases were adjusted so that fitted amplitude values are positive, and phase values are between π and $-\pi$. *Phase* was calculated in radians, but we report all values in days from the summer solstice. Allen et al. (2018) previously confirmed that this non-linear fitting routine yields parameter values and component standard errors that are equivalent to those obtained by fitting sine curves as an additive model of sine and cosine functions with their uncertainties calculated by Gaussian error propagation. It should be noted that standard errors depend on the length of records, and while some stations have datasets that are as long as 57 years, shorter durations are more common (Figure 2a). We fitted the sine curves by two alternative approaches: a) using iteratively reweighted least squares with a bisquare weighting function (*robust-fitted*), and b) using standard least squares with the influence of each monthly isotope measurement weighted by the amount of precipitation during that month (*amount-weighted*). These metrics have different limitations. The amount-weighted cycles are less influenced by erratic values that can occur in low-precipitation months, but also do not capture the variations during drier seasons as effectively. These metrics have different limitations. For example, if there was an anomalously dry month in a short data record, and that dry month also had an erratic atypical isotope value (e.g., because it was composed of a

4

single small event), that value could result in a robust-fit exaggerating the true seasonal isotope cycle. If estimates based on that sinusoid were later weighted with typical precipitation amounts, this could introduce errors. Weighted-fits could introduce errors if drier season precipitation is important to the study system, but the dry season precipitation has minimal influence on the fits and thus those values are misrepresented. Weighted fits might also mischaracterize the seasonal dynamics of a typical year in regions that are impacted by extreme precipitation in some years (e.g. hurricanes or monsoons) if that extreme precipitation has distinct isotope values and yields volumes that are substantial fractions of annual precipitation (e.g., Price et al., 2008). We focus on the robust-fitted parameters describing the seasonal cycles, but for comparison, the amount-weighted fits are also reported in Supporting Information 2. We recommend that future users of these data carefully consider their different limitations when selecting between these two approaches.

2.3.

Precipitation sinusoidal prediction methods

To characterize spatial variations in precipitation isotope seasonality, we establish relationships between the fitted sine parameters (*amplitude*, *phase*, and *offset*) and site characteristics of the precipitation isotope monitoring stations using multiple linear regression. To characterize the monitoring stations, we used elevation, absolute latitude, distance from the nearest ocean, mean annual temperature, range of mean monthly temperatures, seasonal amplitude of precipitation amount, and mean annual precipitation amount (Figure 1). We chose these metrics as spatial predictors because global datasets of these metrics are publicly available and they capture aspects of climate and circulation patterns that are known to affect precipitation isotopic composition (Aggarwal et al., 2016; Birks and Edwards, 2009; Rozanski et al., 1993). To determine which predictors should be included in regression models, we used a stepwise model selection approach in which different combinations of predictors were used to maximize R^2 values while requiring that all coefficient p-values are statistically significant ($p < 0.05$). This step limits model overfitting by excluding redundant or non-significant predictors. We found that using these criteria more aggressively removed variables compared to the more standard Akaike Information Criterion (AIC). To assess collinearity among these variables, we calculated the variance inflation factors (VIF) associated with a hypothetical model that includes all six variables; we found those factors to range from 1.4 to 7.8, and while no fitted models actually included all six terms, the variance inflation factors among the six predictors are still all below the often-used threshold of 10 (Marquaridt, 1970). After identifying the appropriate model terms, models were fitted using the "fitlm" function with robust fitting options that reduce the influence of outliers (MATLAB R2016B). In preliminary analyses, we also tested other metrics – precipitation phase, temperature phase, and mean daily temperature range – but determined that they were not consistently important (i.e., when included in the initial model selection, they were mostly excluded). Thus we excluded these other metrics from subsequent analyses to avoid overcomplicating the models; however, they often showed interesting relationships with the sine parameters, so they are provided in Figure S1.

5

For models of phase, we only used data from monitoring stations where there is a distinct seasonal cycle, because phase terms are meaningless and fitted values are unstable where there are no sinusoidal seasonal cycles; these phase values will also be excluded from the supporting information data files to avoid confusion. We characterize distinct seasonal cycles as ones where

5   the phase is well constrained, with standard errors of the fitted phase terms lower than 15 days (and thus 95 % confidence intervals of approximately ± 1 month). Roughly 74 % of the sites ($n = 479$) met this criterion. We also tested other criteria for filtering out stations with meaningless phase terms, such as $R^2 > 0.3$ ($n = 425$) or $R^2 > 0.5$ ($n = 232$), and those yielded similar regression models for phase. We modelled phase in mid and high latitudes (30° to 90°; $n = 349$ after removing data without distinct seasonal cycles) separately from phase in tropical and subtropical latitudes (0° to 30°; $n = 130$ after removing data

10 without distinct seasonal cycles). We took this approach because initial inspections of these data and past examinations of similar data (Bowen and Revenaugh, 2003; Feng et al., 2009; Halder et al., 2015) suggested that phase is relatively consistent within each of these zones, with sharp transitions at approximately 30° N and S (roughly corresponding with Hadley Cell boundaries; Birner et al., 2014).

15 These fitted spatial regression equations for *amplitude*, *phase*, and *offset* were used to map global precipitation isotope seasonality using the gridded site-characteristic data. We did not extend these maps to extrapolate Antarctic isotope seasonality because there are few monitoring stations there. We also mapped the residuals, estimated by subtracting the regression model estimates of *amplitude*, *phase*, and *offset* from the same variables determined from the fitted sine curves at the precipitation monitoring stations. We interpolated those residuals using inverse-distance weighting of the residual values from the three

20 stations that are most proximal to each grid-cell centre. For phase, we used nearest neighbour interpolation, rather than inverse-distance weighting, because averages across unlike phases are poorly representative. We then applied a Gaussian filter to smooth the each of the residual adjustment layers, with the standard deviation equal to 3°, because we assume there are measurement uncertainties and thus the layer should not be fitted exactly to the points. For phase, we used nearest neighbour interpolation, rather than inverse-distance weighting, because averages across unlike phases are poorly representative; also,

25 we smoothed the phase residuals separately in absolute latitudes > 30° versus absolute latitudes < 30°. For final predictive maps, we added the smoothed residual maps to the regression-based maps; wherever negative amplitudes were resulted, those values were forced to zero. Errors were evaluated by running this routine again, but with while randomly excludingsetting aside 10% of the sites (65 sites (10%)) to not use in the calibration so that they could be usedfor subsequent use as independent quality-control checks. Sine parameters for those 65 stations were predicted using models calibrated with the other ~585 sites;

30 this Monte Carlo procedure was iterated 15 times for both $\delta^{18}O$ and δ^2H.

We provide these predictive maps of the gridded amplitude, phase and offset values of $\delta^{18}O$ and δ^2H. We also provide gridded amplitude, phase, and offset values for precipitation amount, which can be used to scale precipitation isotopic inputs, in

6

applications where amount is important. These maps are provided ~~as geoTIFF files~~ with georeferencing metadata (Supporting Information 3).

To explore sub-global variations in performance of the spatial multiple regression models, we also performed regional regression analyses in which we fitted multiple regressions to data from subsections of the globe. Regressions of *amplitude*, *phase*, and *offset* were calculated for 40° × 40° windows using the same site characteristics that were used in the global models: absolute latitude, elevation above sea level, distance from coastline, range of mean monthly temperatures, mean annual temperature, and annual precipitation amount. These regional regressions were calculated at all vertices of a 10° grid (marking the centre of each 40° window). We used the same combination of stepwise regression model selection and robust regression fitting as in the global analysis. Only windows that contained more than 25 precipitation isotope monitoring stations were analysed. We report gridded R^2 and root mean square error (RMSE) values to indicate where these relationships are strongest. We also provide fitted sine parameters and site characteristics in the supporting information to facilitate users' development of other regression models for regionally specific applications (Supporting Information 2).

3 Results

3.1 Seasonal cycles in precipitation isotopes

Globally, 94 % of the precipitation $\delta^{18}O$ monitoring stations (n = 650) have statistically significant seasonal isotope cycles ($p < 0.05$; t-test of the $\delta^{18}O$), although those cycles do not always explain the majority of the variance in monthly isotope values (i.e., only 36 % of the stations had R^2 greater than 0.5; Figure 2). Amplitudes range from 0 to 11 ‰ $\delta^{18}O$ (~~Figure 2~~Figure 3), with a median value of 2.3 ‰ $\delta^{18}O$; here, amplitude quantifies the strength of seasonal cycles as deviations from average annual values, so an amplitude of 2.3 ‰ $\delta^{18}O$ corresponds to a range of 4.6 ‰ between typical values in the "higher $\delta^{18}O$ season" and the "lower $\delta^{18}O$ season". Seasonal isotope variations are larger in colder, higher-latitude, higher-elevation, or more continental regions (~~Figure 2~~Figure 3), although no individual site characteristic explains the majority of variation in amplitude (~~Figure 2~~Figure 3; Table 1). The few coastal stations that have strong seasonal cycles are almost exclusively located in high absolute-latitude regions (~~Figure 3~~Figure 4a). ~~To our surprise, m~~Many of the monitoring sites within tropical latitudes also have substantial seasonal cycles; for example, 27 % of sites in the tropics show amplitudes greater than 3 ‰ $\delta^{18}O$, and they are not all high-elevation sites (~~Figure 2~~Figure 3b).

Although most stations show a seasonal precipitation $\delta^{18}O$ cycle, the ability of sine curves to capture monthly $\delta^{18}O$ values varies (Figure 2). The median percent of variance explained by sine curves is 42 %; the median RMSE of individual monthly deviations from fitted sine curves is 2.2 ‰ $\delta^{18}O$. Stronger fits occur where a) there is a strong seasonal cycle, b) the seasonal cycle is the dominant pattern of variation, and c) sine curves are the appropriate shape to characterize precipitation isotope

7

variations. Accordingly, the spatial pattern in R^2 (Figure ~~2~~S1c) is broadly similar to the pattern in amplitude ($r = 0.74$). However, RMSE also increases with amplitude ($r = 0.58$), demonstrating that greater seasonal variability is also generally associated with greater month-to-month deviations from the seasonal sinusoidal cycle.

5   The phase term is well constrained (i.e., SE of phase < 15 days) at most but not all sites ($n = 479$), and its geographic distribution is surprisingly binary (~~Figure 3~~Figure 4b). From 30° S to 30° N (i.e., roughly corresponding with the Hadley cells), peak isotope values occurred 104 ± 43 days before the summer solstice (mean $\pm$ SD). By contrast, in the mid- and high-latitude regions, peak isotope values occurred 18.6 ± 24 days after the summer solstice. A few exceptions are found in absolute latitudes near 30°, which may be attributable to the effects of the Asian monsoon cycle (Cai et al., 2018) or the migration of Hadley cell

10   boundaries, which do not consistently occur at 30° (Chen et al., 2014). Peak precipitation isotope values occur within a month of peak temperature at ~~68~~89 % of the monitoring stations that are in absolute latitudes above 30° and have well-constrained seasonal isotopic phases (Figure S~~2~~3)~~.~~; h~~H~~owever, ~~this~~ that pattern was not ubiquitous. On average, phase of δ^2H significantly lags δ^{18}O in absolute latitudes over 30° (p < 0.01), albeit with a median difference of only 2 days (and median absolute difference of 4 days); these observations suggest that precipitation LC-excess, defined as δ^2H–$a\times\delta^{18}$O−b (where a is the slope

15   and b is the intercept of the LMWL; Landwehr and Coplen, 2006), ~~may~~ frequently ~~has~~ have a seasonal cycle ~~and thus an elliptical LMWL~~, as previously described in Switzerland (Allen et al., 2018) and suggested in global deuterium-excess variations (Pfahl and Sodemann, 2014).~~.~~

Offset values, describing the central tendency of the seasonal cycle, span a range of 33 ‰ in δ^{18}O. These values are highest

20   (least negative) in tropical and subtropical regions, and lowest in polar regions (~~Figure 3~~Figure 4c). Most prominent is the strong temperature trend (0.47 ‰ δ^{18}O per °C, $R^2 = 0.77$; ~~Figure 2~~Figure 3; Table 1), consistent with patterns that have been previously described (Dansgaard, 1964; Rozanski et al., 1993). It should be noted that offsets and amplitudes are associated differently with continentality (~~Figure 3~~Figure 4 a,c); while many of the regions with highly negative offsets also have large amplitudes, this is untrue of coastal regions in mid and high latitudes where highly negative offsets and small amplitudes co-

25   occur. For example, in Reykjavik, Iceland, the δ^{18}O offset is -8.0 ‰ and the amplitude is 0.9 ‰; a similar offset is found in continental Iowa, USA (-8.2 ‰), but the amplitude is 4.5 times larger (4.0 ‰).

3.2 Spatial patterns in parameters describing precipitation isotopic cycles

The spatial patterns in amplitude, phase, and offset can be described as functions of site characteristics. Of the predictors

30   examined, all have significant correlations (at p < 0.05) with amplitude, phase, and offset (Table 1; see also ~~Figure 2~~Figure 3). Spearman rank correlations, which are less influenced by extreme values, are also statistically significant for all but one of

these relationships (Table 1). However, no variables explain the majority of variation in amplitude, and only temperature explained the majority of variation in offsets (Table 1).

We developed multiple linear regression models of site characteristics and sine parameters, and used them to generate maps
5   of $\delta^{18}O$ sinusoidal cycles (~~Figure 3~~Figure 4). The multiple regression models explain 64 % of the variation in amplitude (RMSE = 1.1 ‰) and 83 % of the variation in offset (RMSE = 2.0 ‰). The multiple regression models for phase have low R^2 values (0.19 and 0.21, respectively for absolute latitudes above and below 30°) because there is little variation in phase within each latitude band; thus, phase RMSE values are small (12 and 28 days; Table 2). The coefficients of the multiple regression equations describing mapped precipitation $\delta^{18}O$ sinusoidal cycles are presented in Table 2 and analogous coefficient tables
10   describing global regression models of δ^2H, amount-weighted $\delta^{18}O$, and amount-weighted δ^2H cycles are presented in Table S1.

Residuals from the interpolated sine parameter layers are often ~~clustered~~ show clusters of similar values (~~Figure 4~~Figure 5), implying that sources of geographic variation are not fully captured by the predictors that we have used. Consequently,
15   regionally calibrated models (calculated over moving 40° × 40° windows) often yield better fits (~~Figure 5~~Figure 6). Even in regions where multiple regression models do not effectively explain the variations in precipitation isotope sine parameters (e.g., Central America, South-central Asia), they will necessarily be fitted to the mean regional values, so the regional multiple regression model errors (RMSEs) will usually be smaller than those of the global regression model.

20   To produce final predictive maps, we adjusted for the geospatially clustered residuals by adding the smoothed residual maps (~~Figure 4~~Figure 5) to the regression-based maps (~~Figure 3~~Figure 4). These predictive sinusoidal maps of $\delta^{18}O$ seasonality (~~Figure 6~~Figure 7) and δ^2H seasonality (Figure S~~3~~4) are made available in the supplementary materials. They capture 88 %, 97 %, and 96 % of the global variations in amplitude, phase, and offset, respectively. To calculate the prediction errors, we ran this routine again, but randomly excluded~~set aside~~ 10% of the sites ~~to not use in~~from the calibration so that the sine parameters
25   at those sites were predicted independently; the median amplitude and offset errors were 0.49 ‰ and 0.73 ‰ $\delta^{18}O$ (and 4.0 ‰ and 7.4 ‰ δ^2H), and median phase errors were 8 and 20 days (respectively for absolute latitudes above and below 30°).

4 Discussion

The occurrence of seasonal cycles in precipitation isotopes enables tracking how precipitation cycles propagate through landscapes and ecosystems. Previous research has found that precipitation isotopes vary seasonally, and that these seasonal
30   patterns vary geographically (Halder et al., 2015; Rozanski et al., 1993). This work quantifies those seasonal patterns and their

geographical variation, yielding global maps of sinusoidal precipitation isotope cycles (i.e., global sinusoidal 'isoscapes') that can be used to predict seasonal precipitation isotope cycles in sites or regions where they have not been measured.

Site characteristics explain most of the global precipitation isotope cyclicity, albeit with uncertainty in the regression model, the sine fits, and the raw data. Amplitude variations are mostly predictable by multiple regression (Table 2), but there were regional clusters of substantive (±1-2 ‰ δ^{18}O) amplitude residuals. For example, the regression model (~~Figure 3~~Figure 4) tended to systematically underestimate amplitudes in Canada and the northern United States, and systematically overestimate amplitudes in other regions (e.g., Southeast USA, East Asia, and East Africa). We partially mitigated these discrepancies between model outputs and observations by interpolating and smoothing the residuals, as commonly done for precipitation isotope maps to improve the fit of the maps to the data (e.g., Terzer et al., 2013). Better fits could have been achievable through using more predictor variables in the regression models, however we chose to limit the number of variables in the multiple regression models, even prior to the stepwise model selection; while we explored new relationships between precipitation isotope seasonality and (for example) diel temperature range or precipitation amount seasonality (Figure S1~~2~~), these offer little explanatory power that is not also captured in simpler metrics. Regardless, some uncertainties are introduced by using gridded climate products to infer site characteristics, because grid-cell means are not always representative of individual station locations, as demonstrated by the mismatch between the elevations of monitoring stations and the mean elevations of the pixels they occupy (Figure S4~~5~~). Other uncertainties in the regression predictions likely result from errors in the initial sine-curve fitting, as demonstrated by the fact that the regression models improve when only stations with longer records are used. For example, if we exclude all datasets shorter than three years (see Figure 2a), the R^2 of the δ^{18}O amplitude model increases from 0.64 to 0.73 and the R^2 of the offset model increases from 0.83 to 0.87. Any uncertainties in the models or the underlying data, however, do not preclude widespread estimation of precipitation stable isotope cycles at the level of confidence indicated (e.g., in Table 2 and ~~Figure 4~~Figure 5, or Figure 2S1b), which is improved upon through use of the residual-adjusted maps. Predictions can also be improved by using multiple regression models calibrated across individual regions of interest (using the data in Supporting Information 2).

These maps support predicting seasonal isotope cycles, but seasonal isotope cycles are only sometimes useful for predicting individual-month isotope values. To predict individual-month isotope values from a sine curve, the sine curve must be predictable (e.g., with well-constrained phase value), but also the sine curve must capture monthly isotope variations (e.g., R^2 must be high). In only a small subset of the monitoring stations were R^2 values consistently high (Figure 2S1c). For example, at only 6 % of stations was more than 75 % of the variance explained by sine curves. Even fewer stations had long time series that enabled us to determine whether the high R^2 values also imply that inter-annual variations are small (e.g., such as in continental or northern latitude monitoring stations; Figure 2S1a). Thus, individual month values should be carefully inferred

from sine curves (e.g., by assuming errors of magnitudes like those shown in ~~Figure S1~~Figure 2b), even where precipitation isotope ~~cycles~~ seasonality ~~is~~are predictable.

5 Precipitation isotope cycles are likely to be least predictable ~~at~~in latitudes near 30°S, 0°, ~~and~~or 30°N, where our models abruptly shift in phase, approximately demarcating global atmospheric circulation patterns. However, the inter-tropical convergence zone (ITCZ) is not consistently at 0° and Hadley cell boundaries are not consistently at 30°S and 30° N (in space or time; Birner et al., 2014; Chen et al., 2014), which may explain why most of the poor phase predictions (~~Figure 4~~Figure 5b) occur near 30° N or S. There are also errors near 0°, where predicted phase values differ by six months on either side of the

10 equator, which does not precisely demarcate the ITCZ and relevant atmospheric circulations. Bowen et al. (2005) recognized this ITCZ effect and instead used the mean ITCZ position, rather than 0°, to account for phase shifts that occur there; although adopting Bowen's approach ~~c~~should mitigate some of the anomalies at 0° and 30° (~~Figure 4~~Figure 5), other issues in predicting phase would persist (e.g., the elimination of higher frequency cycles; Jacobs et al., 2018). Thus, we opt for our simpler approach and accept that our model is sometimes uncertain in zones near 0° and 30°, although those uncertainties are partially mitigated

15 in the residual-adjusted maps.

~~Precisely predicting precipitation isotope cycles in low latitudes may require consideration of circulation patterns and their temporal variability (Cai et al., 2018; Martin et al., 2018), or use of regional multiple regression equations (which performed well in those regions; Figure 5). Precisely predicting precipitation isotope cycles in low latitudes may require consideration of circulation patterns and their temporal variability (Cai et al., 2018; Martin et al., 2018), or use of regional multiple regression~~

20 ~~equations (which performed well in those regions; Figure 5).~~

Shortcomings in regression models may also result from not accounting for storm trajectories ~~nor~~or convective effects, both of which influence precipitation isotope ratios (Aggarwal et al., 2016; Hu et al., 2018; Konecky et al., 2019). Models representing those processes can aid in interpreting or predicting stable isotope ratios (Hu et al., 2018; Risi et al., 2010).

25 Furthermore~~,~~, ~~and~~ ~~storm sources and cloud types are a likely cause of~~ the ~~the~~ variability in tropical precipitation isotopes ratios we show here may be the result of different storm sources and cloud types (Bailey et al., 2017; Scholl et al., 2009) ~~that we~~ ~~show here.~~ ~~that we describe here.~~Thus, ~~P~~precisely predicting precipitation isotope cycles in low latitudes without calibration data may (especially) require consideration of circulation patterns and their temporal variability (Cai et al., 2018; Martin et al., 2018b)~~;~~ an alternative option would be using ~~, or use of~~regional multiple regression equations, which ~~(which p~~performed well

30 in those regions~~;~~ (Figure 6). ~~Nonetheless~~Regardless, most systematic effects should be compensated by the residual-smoothing step, as demonstrated by the relatively small prediction errors that we observed.

11

The 653 isotope monitoring stations used here span much of earth's climatic heterogeneity, but not all regions. The distributions of the site characteristics associated with these 653 monitoring stations are roughly similar to the global distributions of those characteristics (Figure S5~~6~~). However, high-latitude, high-elevation monitoring stations are scarce (Figure S6~~7~~). More notably, measurements are absent in large regions of Africa, Australia, central Asia, and north Asia. The most interior regions of continents generally contained the fewest monitoring stations (Figure 1b), and we suspect that our regression equations may underestimate the true increase in amplitude with distance from oceans (e.g., see amplitude underestimates in continental North America; ~~Figure 3~~Figure 4a). New precipitation isotope monitoring stations would help fill in important gaps.

These maps of seasonal precipitation isotope cycles serve as tools for studying terrestrial processes. In regions where seasonal precipitation isotope dynamics are well described by sine curves, sinusoidal isotope models are useful for predicting isotope ~~cycles~~ values either at explicit points or continuously in time and space. The presence of large seasonal isotope cycles also enables the quantification of mixing, transport, and turnover of water (or its constituent O and H) in landscapes or biota. This is possible because 1) amplitude dampening reflects mixing processes, 2) phase shifts reflect advective travel times, and 3), offset differences reflect proportional contributions of different seasons' precipitation. In hydrology, the proportion of recent precipitation in streams can be estimated as the ratio of precipitation and streamwater isotope amplitudes (i.e., the young water fraction; Kirchner, 2016a). Maps of precipitation isotope cycles can facilitate estimating average precipitation amplitudes across catchments (Dutton et al., 2005; Jasechko et al., 2016). In such cases isotope values should ideally be weighted by precipitation amount, to diminish the influence of low volumes (von Freyberg et al., 2018). Quantifying seasonal precipitation isotope cycles also facilitates identifying the proportion (and over/under-representation) of precipitation from different seasons in samples such as ~~streamwater~~ surface waters (Bowen et al., 2019; DeWalle et al., 1997; Halder et al., 2015)~~(DeWalle et al., 1997; Halder et al., 2015)~~, groundwater (Jasechko et al., 2014; Kalin and Long, 1994; Lee and Kim, 2007), or plant and soil water (Allen et al., 2019). Similarly, ecological and physiological inferences can be drawn by observing how seasonal variations in water isotope signals are incorporated into (or propagate through) plant and animal tissues (Csank et al., 2016; Gessler et al., 2014; Martin et al., 2018a; Vander Zanden et al., 2015; Yang et al., 2016). Even where phase values are poorly constrained, amplitude and offset values ~~still~~ are still useful identifiers of typical mean values and ~~their~~ magnitudes of seasonal variation. Thus, we expect that the mapped sine parameters that we have developed, as concise characterizations of seasonal precipitation isotope cycles, will find use in both physical and biological sciences.

These maps also indicate where precipitation isotope seasonality should be considered in interpreting isotopic signals in biological and geological samples. Annual mean precipitation may poorly predict the average isotopic input to any biological or geological process that does not integrate precipitation waters throughout entire years, particularly where precipitation

isotopic composition is strongly seasonal (as discussed by, e.g., Dutton et al., 2005). Whereas event-to-event variations are likely to be rapidly damped by mixing in soils, lower-frequency variations, such as seasonal cycles, can persist and propagate through the water cycle. Where uptake and incorporation of isotopes into organisms (Balasse et al., 2003; Schubert and Jahren, 2015) or geologic materials (Johnson et al., 2006) also vary seasonally, mean annual precipitation may poorly and

5   inconsistently approximate their average source water. For example, consider a hypothetical case of soil water with an isotopic composition that is consistently equal to that of the current month's mean precipitation. Further assume that a tree growing in this soil takes up that soil water and incorporates its oxygen atoms into cellulose during the six months of the warm season (e.g., when high-δ^{18}O precipitation falls in high latitudes). For example, if the precipitation δ^{18}O has a seasonal amplitude of 4 ‰, the average composition of the water taken up by the tree will be approximately $(2/\pi$~~*~~$) \times$ 4 ‰ ≈ 2.5 ‰ higher than the

10   annual average precipitation. This bias will be larger in locations where the seasonal amplitude of precipitation isotope cycles is larger. Thus, our maps showing precipitation isotope seasonality can be used to identify locations where such biases are potentially significant.

5 Summary

The majority of stable isotope time series measured at 653 precipitation isotope monitoring stations show significant sinusoidal

15   seasonal cycles in precipitation isotopes. The fitted parameters that define these seasonal precipitation isotope cycles are estimated through multiple regression models of site characteristics. These spatial models enabled us to develop maps that describe global patterns in precipitation isotope seasonality, although regionally calibrated spatial models often better captured regional variations in precipitation isotope seasonality. The global maps and associated fitted isotope data are made available as supplementary information.

Data Availability

25   In Supporting Information 2, we provide all of fitted sine curves and site metadata for the 653 precipitation monitoring stations that are presented in this study. In Supporting Information 3, we provide metadata and a link to a 5-minute resolution gridded amplitude, phase, and offset for δ^{18}O and δ^2H of robust-fitted sine curves, hosted on Zenodo.org. All raw data used are synthesized from other studies or publicly available datasets; contact Dr. Jeff Welker ~~for more information and collaborations~~

13

Supplementary Materials

Supplementary Information 1

5   Table S1 Multiple regression coefficients and fit statistics for models describing the spatial variations in sine parameters that capture seasonal precipitation isotope cycles (amount-weighted fitted $\delta^{18}O$, robust-fitted δ^2H, and amount-weighted fitted δ^2H).

Fig. S1 Maps of precipitation isotope measurement stations' measurement durations and sine-curve goodness-of-fit statistics.

Fig. S12 Scatter plots of fitted sine parameters describing precipitation $\delta^{18}O$ seasonal cycles versus site characteristics that were not included in the regression models.

10   Fig. S23 Histogram of phase differences between seasonal isotope cycles and seasonal temperature cycles.

Fig. S34 Maps of fitted station values (markers) and the residual-adjusted maps of sine-curve parameters (shaded) that describe the seasonal cycles in precipitation $\delta^{18}O$ a) amplitude, b) phase, and c) offset.

Fig. S45 Elevations reported for sites regressed against gridded predictions of elevations of pixels containing those sites.

Fig. S56 Probability density functions of the site characteristics used to predict seasonal precipitation isotope cycles.

15   Fig. S67 Elevation versus latitude of precipitation isotope monitoring sites.

Supplementary Information 2

Data S1 List of fitted $\delta^{18}O$ and δ^2H sine parameter values (robust fitted, and amount-weighted fitted) and site characteristics (to be made available upon acceptance)

20

Supplementary Information 3

Data S2 Information to access the geospatial database (hosted on the public repository Zenodo.org), containing TIFF file of the following gridded products: Data S2 Gridded $\delta^{18}O$ amplitude GeoTIFF file (to be made available upon acceptance); Data S3 Gridded $\delta^{18}O$ phase Geo; TIFF file (to be made available upon acceptance)

25   Data S4 Gridded $\delta^{18}O$ offset ; GeoTIFF file (to be made available upon acceptance)

Data S5 Gridded δ^2H amplitude; GeoTIFF file (to be made available upon acceptance)

Data S6 Gridded δ^2H phase; GeoTIFF file (to be made available upon acceptance)

Data S7 Gridded δ^2H offset; GeoTIFF file (to be made available upon acceptance)

Data S8 Gridded precipitation amount amplitude; GeoTIFF file (to be made available upon acceptance)

30   Data S9 Gridded precipitation amount phase; GeoTIFF file (to be made available upon acceptance)

Data S10 Gridded precipitation amount offset. GeoTIFF file (to be made available upon acceptance)

References

Aggarwal, P. K., Froehlich, K. and Gonfiantini, R.: Contributions of the International Atomic Energy Agency to the development and practice of isotope hydrology, Hydrogeol J, 19(1), 5–8, doi:10.1007/s10040-010-0648-3, 2011.

Aggarwal, P. K., Romatschke, U., Araguas-Araguas, L., Belachew, D., Longstaffe, F. J., Berg, P., Schumacher, C. and Funk, A.: Proportions of convective and stratiform precipitation revealed in water isotope ratios, Nature Geoscience, 9(8), 624–629, doi:10.1038/ngeo2739, 2016.

Allen, S. T., Kirchner, J. W., Braun, S., Siegwolf, R. T. W. and Goldsmith, G. R.: Seasonal origins of soil water used by trees, Hydrology and Earth System Sciences Discussions, 1–23, doi:https://doi.org/10.5194/hess-2018-554, in review.

Allen, S. T., Kirchner, J. W. and Goldsmith, G. R.: Predicting spatial patterns in precipitation isotope ($\delta2H$ and $\delta18O$) seasonality using sinusoidal isoscapes, Geophysical Research Letters, 4859–4868, doi:10.1029/2018GL077458, 2018.

Bailey, A., Blossey, P. N., Noone, D., Nusbaumer, J. and Wood, R.: Detecting shifts in tropical moisture imbalances with satellite-derived isotope ratios in water vapor, Journal of Geophysical Research: Atmospheres, 122(11), 5763–5779, doi:10.1002/2016JD026222, 2017.

Balasse, M., Smith, A. B., Ambrose, S. H. and Leigh, S. R.: Determining Sheep Birth Seasonality by Analysis of Tooth Enamel Oxygen Isotope Ratios: The Late Stone Age Site of Kasteelberg (South Africa), Journal of Archaeological Science, 30(2), 205–215, doi:10.1006/jasc.2002.0833, 2003.

Berghuijs, W. R. and Woods, R. A.: A simple framework to quantitatively describe monthly precipitation and temperature climatology, International Journal of Climatology, 36(9), 3161–3174, doi:10.1002/joc.4544, 2016.

Birks, S. J. and Edwards, T. W. D.: Atmospheric circulation controls on precipitation isotope–climate relations in western Canada, Tellus B: Chemical and Physical Meteorology, 61(3) [online] Available from: https://www.tandfonline.com/doi/abs/10.1111/j.1600-0889.2009.00423.x (Accessed 7 October 2018), 2009.

Birks, S. J. and Gibson, J. J.: Isotope Hydrology Research in Canada, 2003-2007, Canadian Water Resources Journal, doi:10.4296/cwrj3402163, 2013.

Birner, T., Davis, S. M. and Seidel, D. J.: The changing width of Earth's tropical belt, Physics Today, 67(12), 38, doi:10.1063/PT.3.2620, 2014.

15

Bowen, G. J.: Spatial analysis of the intra-annual variation of precipitation isotope ratios and its climatological corollaries, J. Geophys. Res., 113(D5), D05113, doi:10.1029/2007JD009295, 2008.

Bowen, G. J. and Revenaugh, J.: Interpolating the isotopic composition of modern meteoric precipitation, Water Resources Research, 39(10), doi:10.1029/2003WR002086, 2003.

5   Bowen, G. J. and Wilkinson, B.: Spatial distribution of δ18O in meteoric precipitation, Geology, 30(4), 315–318, doi:10.1130/0091-7613(2002)030<0315:SDOOIM>2.0.CO;2, 2002.

Bowen, G. J., Wassenaar, L. I. and Hobson, K. A.: Global application of stable hydrogen and oxygen isotopes to wildlife forensics, Oecologia, 143(3), 337–348, doi:10.1007/s00442-004-1813-y, 2005.

Bowen, G. J., Liu, Z., Vander Zanden, H. B., Zhao, L. and Takahashi, G.: Geographic assignment with
10 stable isotopes in IsoMAP, Methods Ecol Evol, 5(3), 201–206, doi:10.1111/2041-210X.12147, 2014.

Bowen, G. J., Cai, Z., Fiorella, R. P. and Putman, A. L.: Isotopes in the Water Cycle: Regional- to Global-Scale Patterns and Applications, Annual Review of Earth and Planetary Sciences, 47(1), null, doi:10.1146/annurev-earth-053018-060220, 2019.

Cai, Z., Tian, L. and Bowen, G. J.: Spatial-seasonal patterns reveal large-scale atmospheric controls on
15 Asian Monsoon precipitation water isotope ratios, Earth and Planetary Science Letters, 503, 158–169, doi:10.1016/j.epsl.2018.09.028, 2018.

Chen, S., Wei, K., Chen, W. and Song, L.: Regional changes in the annual mean Hadley circulation in recent decades, Journal of Geophysical Research: Atmospheres, 119(13), 7815–7832, doi:10.1002/2014JD021540, 2014.

20 Clow, D. W., Mast, M. A. and Sickman, J. O.: Linking transit times to catchment sensitivity to atmospheric deposition of acidity and nitrogen in mountains of the western United States, Hydrological Processes, 32(16), 2456–2470, doi:10.1002/hyp.13183, 2018.

Csank, A. Z., Miller, A. E., Sherriff, R. L., Berg, E. E. and Welker, J. M.: Tree-ring isotopes reveal drought sensitivity in trees killed by spruce beetle outbreaks in south-central Alaska, Ecological
25 Applications, 26(7), 2001–2020, doi:10.1002/eap.1365, 2016.

Dansgaard, W.: Stable isotopes in precipitation, Tellus, 16(4), 436–468, doi:10.1111/j.2153-3490.1964.tb00181.x, 1964.

Delavau, C., Chun, K. P., Stadnyk, T., Birks, S. J. and Welker, J. M.: North American precipitation isotope (δ18O) zones revealed in time series modeling across Canada and northern United States, Water
30 Resour. Res., 51(2), 1284–1299, doi:10.1002/2014WR015687, 2015.

DeWalle, D. R., Edwards, P. J., Swistock, B. R., Aravena, R. and Drimmie, R. J.: Seasonal isotope hydrology of three Appalachian forest catchments, Hydrological Processes, 11(15), 1895–1906, doi:10.1002/(SICI)1099-1085(199712)11:15<1895::AID-HYP538>3.0.CO;2-#, 1997.

Dutton, A., Wilkinson, B. H., Welker, J. M., Bowen, G. J. and Lohmann, K. C.: Spatial distribution and seasonal variation in 18O/16O of modern precipitation and river water across the conterminous USA, Hydrol. Process., 19(20), 4121–4146, doi:10.1002/hyp.5876, 2005.

Feng, X., Faiia, A. M. and Posmentier, E. S.: Seasonality of isotopes in precipitation: A global perspective, Journal of Geophysical Research: Atmospheres, 114(D8), doi:10.1029/2008JD011279, 2009.

Fick, S. E. and Hijmans, R. J.: WorldClim 2: new 1-km spatial resolution climate surfaces for global land areas, International Journal of Climatology, 37(12), 4302–4315, doi:10.1002/joc.5086, 2017.

v. Freyberg, J., Allen, S. T., Seeger, S., Weiler, M. and Kirchner, J. W.: Sensitivity of young water fractions to hydro-climatic forcing and landscape properties across 22 Swiss catchments, Hydrology and Earth System Sciences, 22(7), 3841–3861, doi:https://doi.org/10.5194/hess-22-3841-2018, 2018.

Gessler, A., Ferrio, J. P., Hommel, R., Treydte, K., Werner, R. A. and Monson, R. K.: Stable isotopes in tree rings: towards a mechanistic understanding of isotope fractionation and mixing processes from the leaves to the wood, Tree Physiol, 34(8), 796–818, doi:10.1093/treephys/tpu040, 2014.

Halder, J., Terzer, S., Wassenaar, L. I., Araguás-Araguás, L. J. and Aggarwal, P. K.: The Global Network of Isotopes in Rivers (GNIR): integration of water isotopes in watershed observation and riverine research, Hydrol. Earth Syst. Sci., 19(8), 3419–3431, doi:10.5194/hess-19-3419-2015, 2015.

Hu, J., Emile-Geay, J., Nusbaumer, J. and Noone, D.: Impact of Convective Activity on Precipitation δ18O in Isotope-Enabled General Circulation Models, Journal of Geophysical Research: Atmospheres, 123(23), 13,595-13,610, doi:10.1029/2018JD029187, 2018.

Jacobs, S. R., Timbe, E., Weeser, B., Rufino, M. C., Butterbach-Bahl, K. and Breuer, L.: Assessment of hydrological pathways in East African montane catchments under different land use, Hydrology and Earth System Sciences, 22(9), 4981–5000, doi:https://doi.org/10.5194/hess-22-4981-2018, 2018.

Jasechko, S., Birks, S. J., Gleeson, T., Wada, Y., Fawcett, P. J., Sharp, Z. D., McDonnell, J. J. and Welker, J. M.: The pronounced seasonality of global groundwater recharge, Water Resources Research, 50, 8845–8867, doi:10.1002/2014WR015809, 2014.

Jasechko, S., Kirchner, J. W., Welker, J. M. and McDonnell, J. J.: Substantial proportion of global streamflow less than three months old, Nature Geosci, 9(2), 126–129, doi:10.1038/ngeo2636, 2016.

Jasechko, S., Wassenaar, L. I. and Mayer, B.: Isotopic evidence for widespread cold-season-biased groundwater recharge and young streamflow across central Canada, Hydrological Processes, 31(12), 2196–2209, doi:10.1002/hyp.11175, 2017.

Johnson, K. R., Hu, C., Belshaw, N. S. and Henderson, G. M.: Seasonal trace-element and stable-isotope variations in a Chinese speleothem: The potential for high-resolution paleomonsoon reconstruction, Earth and Planetary Science Letters, 244(1), 394–407, doi:10.1016/j.epsl.2006.01.064, 2006.

Kalin, R. M. and Long, A.: Application of hydrogeochemical modelling for validation of hydrologic flow modelling in the Tucson basin aquifer, Arizona, United States of America, International Atomic Energy Agency, Proceedings of a final research co-ordination meeting held in Vienna, 1-4 June 1993. [online] Available from: http://inis.iaea.org/Search/search.aspx?orig_q=RN:26036831 (Accessed 29 January 2019), 1994.

Kirchner, J. W.: Aggregation in environmental systems – Part 1: Seasonal tracer cycles quantify young water fractions, but not mean transit times, in spatially heterogeneous catchments, Hydrol. Earth Syst. Sci., 20(1), 279–297, doi:10.5194/hess-20-279-2016, 2016a.

Kirchner, J. W.: Aggregation in environmental systems – Part 2: Catchment mean transit times and young water fractions under hydrologic nonstationarity, Hydrol. Earth Syst. Sci., 20(1), 299–328, doi:10.5194/hess-20-299-2016, 2016b.

Konecky, B. L., Noone, D. C. and Cobb, K. M.: The Influence of Competing Hydroclimate Processes on Stable Isotope Ratios in Tropical Rainfall, Geophysical Research Letters, 46(3), 1622–1633, doi:10.1029/2018GL080188, 2019.

Landwehr, J. M. and Coplen, T. B.: Line-conditioned excess: A new method for characterizing stable hydrogen and oxygen isotope ratios in hydrologic systems, [online] Available from: http://inis.iaea.org/Search/search.aspx?orig_q=RN:37043527 (Accessed 13 September 2017), 2006.

Lee, K.-S. and Kim, Y.: Determining the seasonality of groundwater recharge using water isotopes: a case study from the upper North Han River basin, Korea, Environmental Geology, 52, 853–859, doi:10.1007/s00254-006-0527-3, 2007.

Lutz, S. R., Krieg, R., Müller, C., Zink, M., Knöller, K., Samaniego, L. and Merz, R.: Spatial Patterns of Water Age: Using Young Water Fractions to Improve the Characterization of Transit Times in Contrasting Catchments, Water Resources Research, 54(7), 4767–4784, doi:10.1029/2017WR022216, 2018.

Marquaridt, D. W.: Generalized Inverses, Ridge Regression, Biased Linear Estimation, and Nonlinear Estimation, Technometrics, 12(3), 591–612, doi:10.1080/00401706.1970.10488699, 1970.

Martin, J., Looker, N., Hoylman, Z., Jencso, K. and Hu, J.: Differential use of winter precipitation by upper and lower elevation Douglas fir in the Northern Rockies, Global Change Biology, 24(12), 5607–5621, doi:10.1111/gcb.14435, 2018a.

Martin, N. J., Conroy, J. L., Noone, D., Cobb, K. M., Konecky, B. L. and Rea, S.: Seasonal and ENSO Influences on the Stable Isotopic Composition of Galápagos Precipitation, Journal of Geophysical Research: Atmospheres, 123(1), 261–275, doi:10.1002/2017JD027380, 2018b.

Pfahl, S. and Sodemann, H.: What controls deuterium excess in global precipitation?, Climate of the Past, 10(2), 771–781, doi:https://doi.org/10.5194/cp-10-771-2014, 2014.

Price, R. M., Swart, P. K. and Willoughby, H. E.: Seasonal and spatial variation in the stable isotopic composition ($\delta18O$ and δD) of precipitation in south Florida, Journal of Hydrology, 358(3), 193–205, doi:10.1016/j.jhydrol.2008.06.003, 2008.

Risi, C., Bony, S., Vimeux, F. and Jouzel, J.: Water-stable isotopes in the LMDZ4 general circulation model: Model evaluation for present-day and past climates and applications to climatic interpretations of tropical isotopic records, Journal of Geophysical Research: Atmospheres, 115(D12), doi:10.1029/2009JD013255, 2010.

Rozanski, K., Araguás-Araguás, L. and Gonfiantini, R.: Isotopic Patterns in Modern Global Precipitation, in Climate Change in Continental Isotopic Records, edited by P. K. Swart, K. C. Lohmann, J. Mckenzie, and S. Savin, pp. 1–36, American Geophysical Union., 1993.

Scholl, M. A., Shanley, J. B., Zegarra, J. P. and Coplen, T. B.: The stable isotope amount effect: New insights from NEXRAD echo tops, Luquillo Mountains, Puerto Rico, Water Resources Research, 45(12), doi:10.1029/2008WR007515, 2009.

Schubert, B. A. and Jahren, A. H.: Seasonal temperature and precipitation recorded in the intra-annual oxygen isotope pattern of meteoric water and tree-ring cellulose, Quaternary Science Reviews, 125, 1–14, doi:10.1016/j.quascirev.2015.07.024, 2015.

Song, C., Wang, G., Liu, G., Mao, T., Sun, X. and Chen, X.: Stable isotope variations of precipitation and streamflow reveal the young water fraction of a permafrost watershed, Hydrological Processes, 31(4), 935–947, doi:10.1002/hyp.11077, 2017.

Terzer, S., Wassenaar, L. I., Araguás-Araguás, L. J. and Aggarwal, P. K.: Global isoscapes for $\delta18O$ and $\delta2H$ in precipitation: improved prediction using regionalized climatic regression models, Hydrology and Earth System Sciences, 17, 4713–4728, doi:https://doi.org/10.5194/hess-17-4713-2013, 2013.

US Geological Survey: Global 30 Arc-Second Elevation (GTOPO30), US Geological Survey, Center for Earth Resources Observation and Science (EROS)., 1996.

Vachon, R. W., White, J. W. C., Gutmann, E. and Welker, J. M.: Amount-weighted annual isotopic (δ18O) values are affected by the seasonality of precipitation: A sensitivity study, Geophys. Res. Lett., 34(21), L21707, doi:10.1029/2007GL030547, 2007.

5 Vander Zanden, H. B., Wunder, M. B., Hobson, K. A., Van Wilgenburg, S. L., Wassenaar, L. I., Welker, J. M. and Bowen, G. J.: Space-time tradeoffs in the development of precipitation-based isoscape models for determining migratory origin, J Avian Biol, 46(6), 658–667, doi:10.1111/jav.00656, 2015.

Welker, J. M.: Isotopic (δ18O) characteristics of weekly precipitation collected across the USA: an initial analysis with application to water source studies, Hydrological Processes, 14(8), 1449–1464, 10 doi:10.1002/1099-1085(20000615)14:8<1449::AID-HYP993>3.0.CO;2-7, 2000.

Welker, J. M.: ENSO effects on δ18O, δ2H and d-excess values in precipitation across the U.S. using a high-density, long-term network (USNIP), Rapid Communications in Mass Spectrometry, 26(17), 1893–1898, doi:10.1002/rcm.6298, 2012.

Wessel, P. and Smith, W. H. F.: A global, self-consistent, hierarchical, high-resolution shoreline 15 database, Journal of Geophysical Research: Solid Earth, 101(B4), 8741–8743, doi:10.1029/96JB00104, 1996.

West, J. B., Bowen, G. J., Dawson, T. E. and Tu, K. P., Eds.: Isoscapes: Understanding movement, pattern, and process on Earth through isotope mapping, Springer Netherlands. [online] Available from: //www.springer.com/gp/book/9789048133536 (Accessed 8 October 2018), 2010.

20 Wilkinson, B. H. and Ivany, L. C.: Paleoclimatic inference from stable isotope profiles of accretionary biogenic hardparts – a quantitative approach to the evaluation of incomplete data, Palaeogeography, Palaeoclimatology, Palaeoecology, 185(1), 95–114, doi:10.1016/S0031-0182(02)00279-1, 2002.

Yang, L. H., Ostrovsky, D., Rogers, M. C. and Welker, J. M.: Intra-population variation in the natal origins and wing morphology of overwintering western monarch butterflies Danaus plexippus, 25 Ecography, 39(10), 998–1007, doi:10.1111/ecog.01994, 2016.

Table 1 Pearson and Spearman correlation coefficients of sine parameters versus (vs.) site characteristics.

Sine parameters	vs. |latitude|	vs. elevation	vs. dist. from coast	vs. temp. range	vs. mean temp	vs. mean precip.
Pearson						
Amplitude	0.34	0.34	0.54	0.58	-0.56	-0.35
Phase	0.76	-0.12	0.25	0.72	-0.68	-0.64
Offset	-0.67	-0.16	-0.23	-0.70	0.88	0.40
Spearman						
Amplitude	0.30	0.42	0.56	0.51	-0.49	-0.37
Phase	0.59	0.04	0.20	0.63	-0.64	-0.62
Offset	-0.69	-0.26	-0.35	-0.65	0.87	0.40

Table 2 Multiple regression coefficients and fit statistics for models describing global variations in sine parameters that capture seasonal precipitation $\delta^{18}O$ cycles. Dashes mark predictors that were excluded by the stepwise-regression model selection.

	|Latitude| (° from equator)	Elevation (m amsl)	Dist. from coast (km)	Temp. range (°C)	Mean Annual Temp. (°C)	Mean Annual Precip. (mm yr^{-1})	Intercept	RMSE	R^2
Amplitude (‰ $\delta^{18}O$)	-0.06	0.0003	0.0013	0.08	-0.12	—	4.5	1.1	0.64
Phase (days)[a]	—	0.005	—	—	-0.38	—	24.2	12.0	0.19
Phase (days)[b]	-1.27	—	—	0.78	—	—	-100.0	28.2	0.21
Offset (‰ $\delta^{18}O$)	0.10	—	—	-0.11	0.55	-0.0008	-15.7	2.0	0.83

[a] referring to sites in latitudes > 30° (N or S)

[b] referring to sites in latitudes < 30° (N or S)
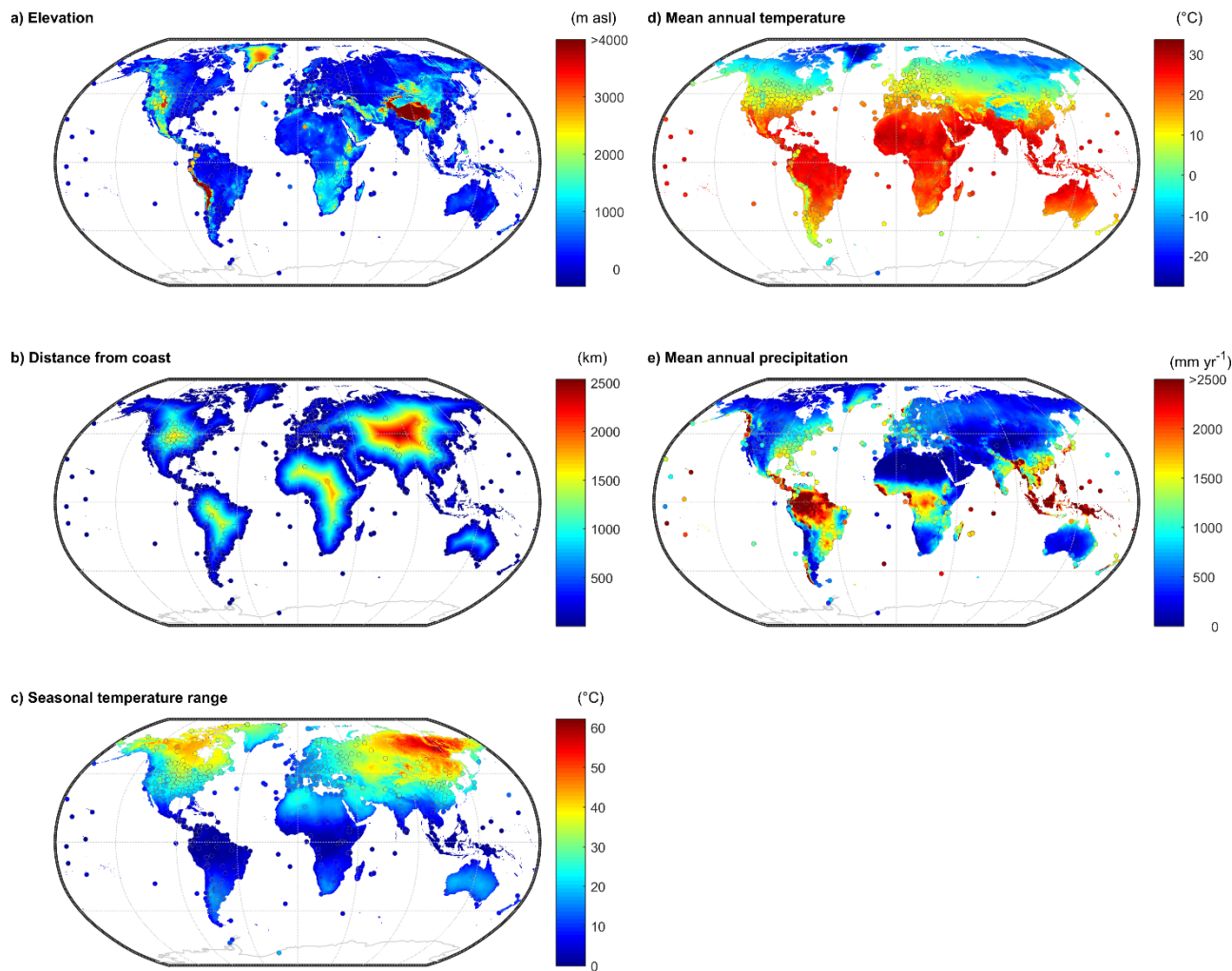
Figure 1 Global maps of site characteristics used for predicting seasonal precipitation isotope cycles: a) elevation of precipitation isotope monitoring stations plotted over the elevation map, b) distance from coast, c) temperature range between mean temperatures of warmest and coldest months, d) mean annual temperature, and e) mean annual precipitation. Values at precipitation isotope monitoring stations are marked by circles. For b-e, station-level data are estimated as the value of the grid cells that the stations occupy.
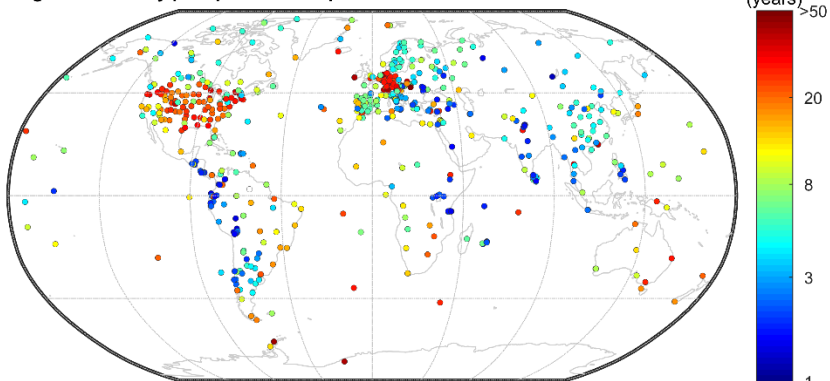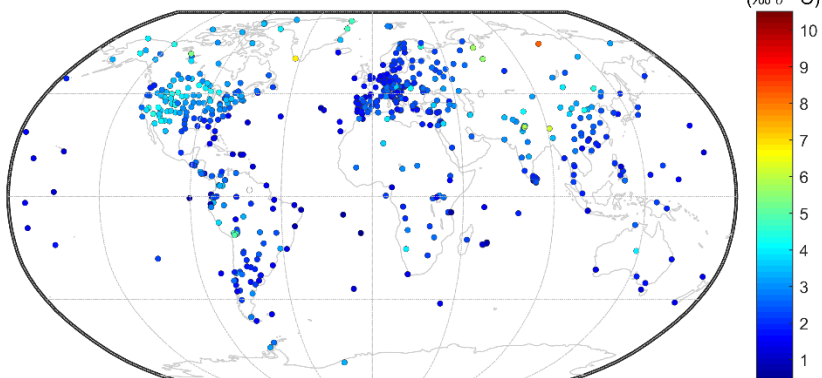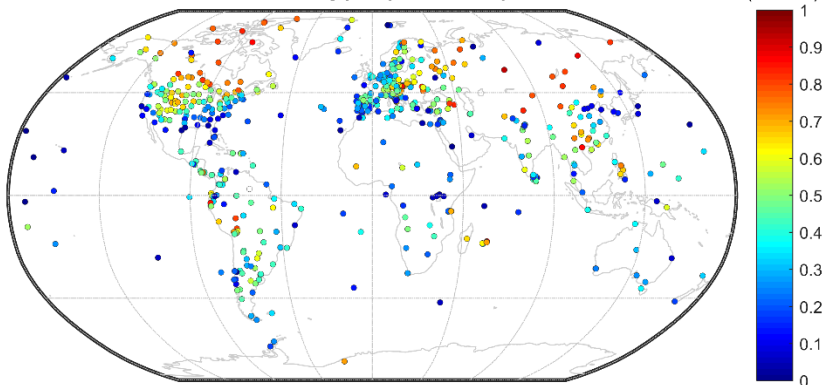
Figure 2. Maps of precipitation isotope measurement stations with colours indicating a) the length of measurements at each site, and goodness-of-fit statistics b) root mean square errors (RMSE) and c) coefficients of variations (R^2) of the fitting of sine curves to monthly, empirical time series from each station. We show the robust-fitted $\delta^{18}O$ statistics; the amount-weighted $\delta^{18}O$ fit statistics, and the δ^2H statistics (robust-fitted and amount-weighted) are provided in the Supporting Information 2 data file.
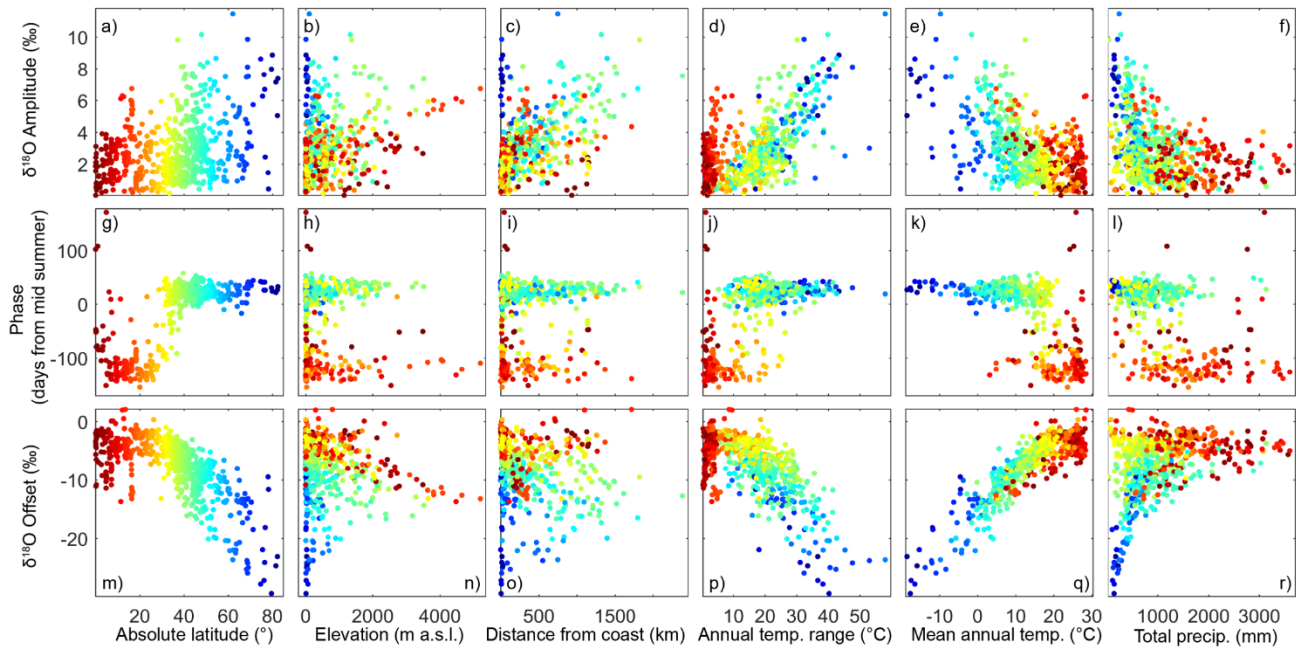
Figure 2Figure 3 Scatter plots of fitted sine parameters describing precipitation δ¹⁸O seasonal cycles – a-f) amplitude, g-l) phase, m-r) offset – versus site characteristics. For associated Spearman and Pearson correlation coefficients, see Table 1. Colours indicate absolute latitude (high latitudes in blue, low latitudes in red) as shown in panels a, g, and m.
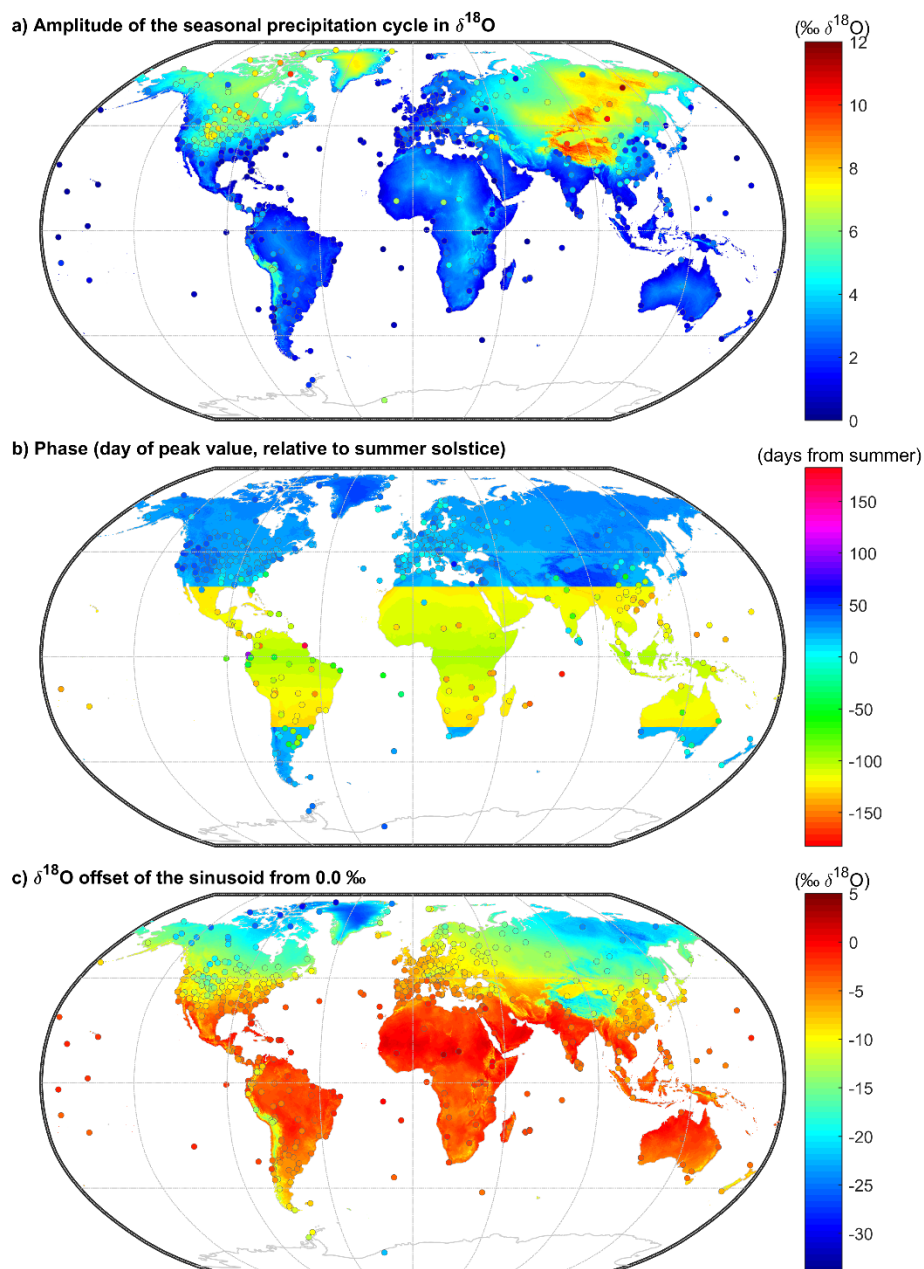
Figure 3Figure 4. Maps of fitted station values (markers) and regression-based sine-curve parameters (shaded) that describe the seasonal cycles in precipitation δ^{18}O a) amplitude, b) phase, and c) offset. The shading reflects multiple-regression models based on landscape characteristics, described in Table 2; for phase, separate models were

26

used in absolute latitudes > 30° versus latitudes < 30° (see methods). Here, residuals were not yet added back into the model.

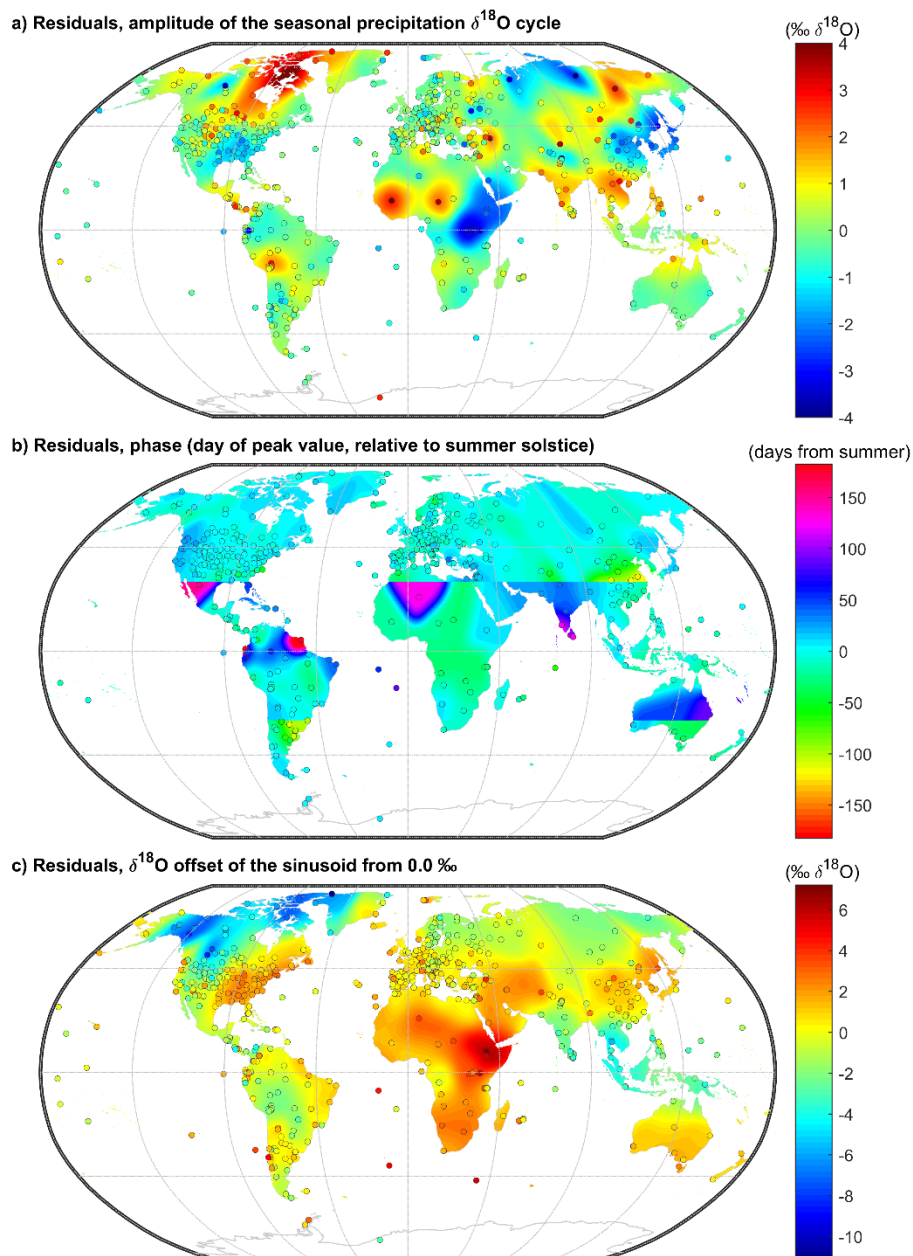**Figure 4Figure 5. Maps of δ¹⁸O a) amplitude, b) phase, and c) offset residuals, where the sine parameter values predicted from the multiple regression equations (shown in the interpolated maps in Figure 3Figure 4) were subtracted from those of parameter values fitted to measurements at each precipitation isotope monitoring site (also shown in Figure 3Figure 4). The shading shows the smoothed residual layers (see Methods).**
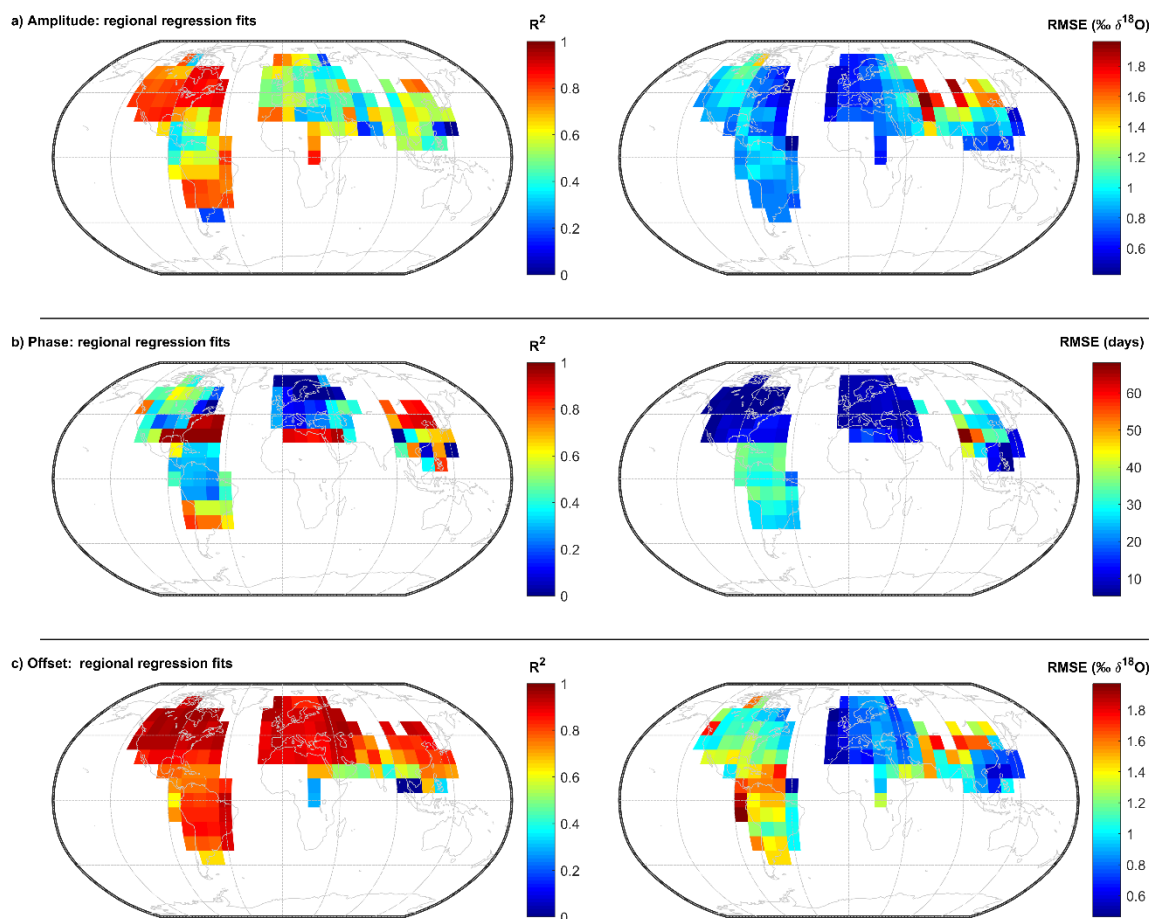
Figure 5Figure 6. Fit statistics for regionally fitted regressions that explain the spatial variations of the precipitation δ¹⁸O sine parameters. Regressions of a) amplitude, b) phase, and c) offset versus site characteristics were calculated for 40° × 40° pixels (centred on vertices at a 10° grid). Only pixels which contained >25 precipitation isotope measurements stations were used; for phase (b), we only used measurement stations that had well-constrained sinusoidal cycles (i.e., the standard error of the phase was less than 15 days). These figures show that site characteristics do not consistently explain the patterns of variations, and often the R^2 values are substantially lower than those of the global regression model (Table 2). However, the errors (RMSEs) are (almost) universally lower than those of the global regression model, implying that regionally calibrated regressions models are better predictors of spatial patterns in precipitation isotope cycles.
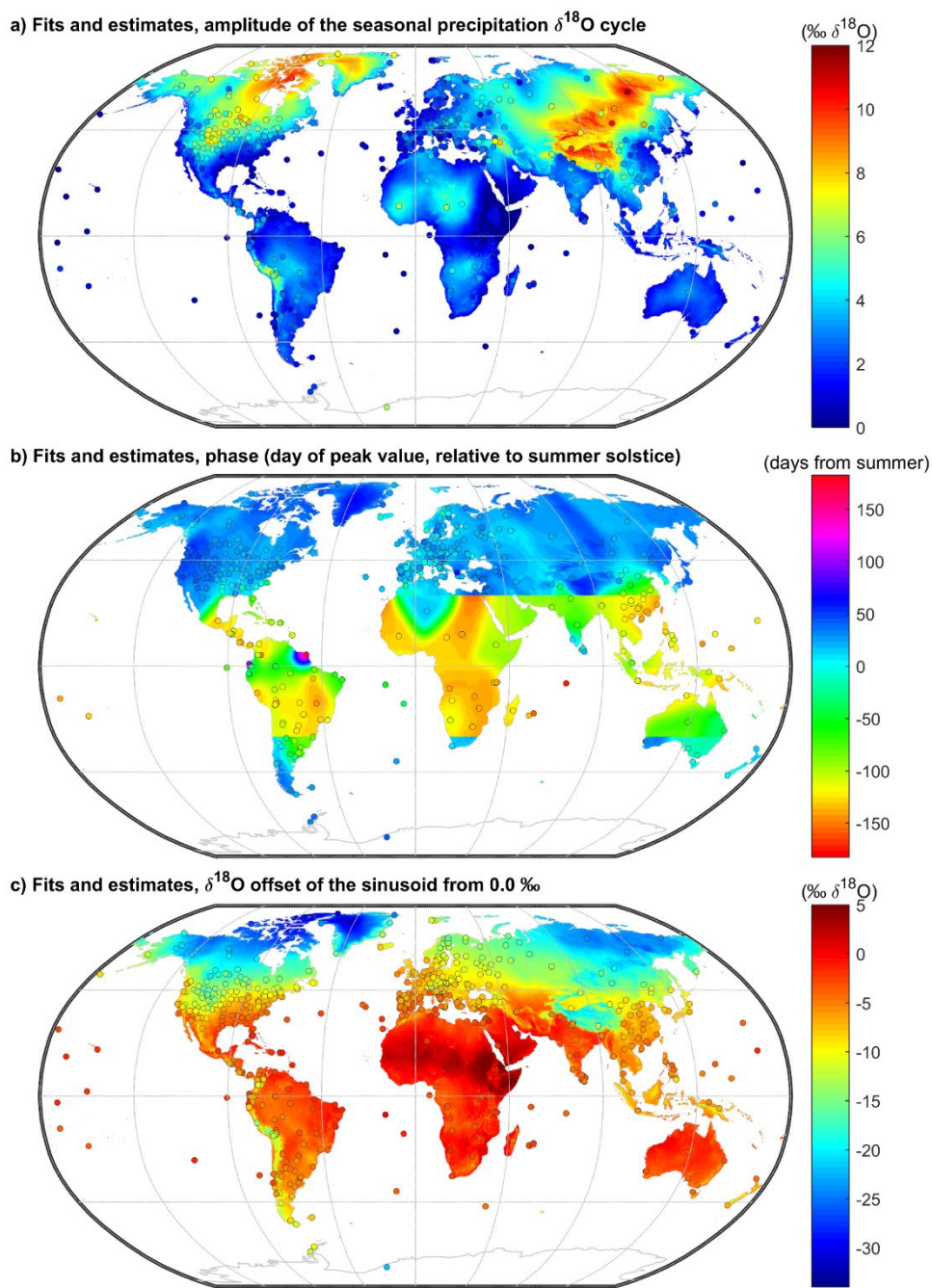
a) Fits and estimates, amplitude of the seasonal precipitation δ^{18}O cycle

b) Fits and estimates, phase (day of peak value, relative to summer solstice)

c) Fits and estimates, δ^{18}O offset of the sinusoid from 0.0 ‰

~~Figure 6~~Figure 7. Maps of fitted station values (markers) and the residual-adjusted maps of sine-curve parameters (shaded) that describe the seasonal cycles in precipitation δ¹⁸O: a) amplitude, b) phase, and c) offset. The interpolated surface is the sum of the infilled surfaces in Figures 3 and 4 (see Methods).